1986-12

Damping degradation in incramute and sonoston due to low temperature storage.

Leary, Lewis William

NAVAL POSTGRADUATE SCHOOL
Monterey, California

THESIS

DAMPING DEGRADATION IN INCRAMUTE AND SONOSTON
DUE TO LOW TEMPERATURE STORAGE

by

Lewis William Leary

December 1986

Thesis Advisor: A.J. Perkins

UNCLASSIFIED
CURITY CLASSIFICATION OF THIS PAGE

REPORT DOCUMENTATION PAGE

REPORT SECURITY CLASSIFICATION UNCLASSIFIED	1b RESTRICTIVE MARKINGS
SECURITY CLASSIFICATION AUTHORITY	3 DISTRIBUTION/AVAILABILITY OF REPORT Approved for public release; distribution is unlimited.
DECLASSIFICATION/DOWNGRADING SCHEDULE	
PERFORMING ORGANIZATION REPORT NUMBER(S)	5 MONITORING ORGANIZATION REPORT NUMBER(S)
NAME OF PERFORMING ORGANIZATION aval Postgraduate School	6b OFFICE SYMBOL (If applicable) 69
7a NAME OF MONITORING ORGANIZATION Naval Postgraduate School	
ADDRESS (City, State, and ZIP Code) onterey, California 93943-5000	7b ADDRESS (City, State, and ZIP Code) Monterey, California 93943-5000
NAME OF FUNDING/SPONSORING ORGANIZATION	8b OFFICE SYMBOL (If applicable)
9 PROCUREMENT INSTRUMENT IDENTIFICATION NUMBER	
ADDRESS (City, State, and ZIP Code)	10 SOURCE OF FUNDING NUMBERS

PROGRAM ELEMENT NO	PROJECT NO	TASK NO	WORK UNIT ACCESSION NO

TITLE (Include Security Classification)
DAMPING DEGRADATION IN INCRAMUTE AND SONOSTON DUE TO LOW TEMPERATURE STORAGE

PERSONAL AUTHOR(S)
LEARY, LEWIS W.

TYPE OF REPORT	13b TIME COVERED	14 DATE OF REPORT (Year, Month, Day)	15 PAGE COUNT
Master's Thesis	FROM _____ TO _____	1986 December	65

SUPPLEMENTARY NOTATION

COSATI CODES		
FIELD	GROUP	SUB-GROUP

18 SUBJECT TERMS (Continue on reverse if necessary and identify by block number)
Damping, Damping degradation, Damping stability, INCRAMUTE, SONOSTON, CU-MN alloys, Specific Damping Capacity (SDC), Resonant dwell technique, Tweed, Microtwins

ABSTRACT (Continue on reverse if necessary and identify by block number)

o commercial manganese-copper based alloys, SONOSTON and INCRAMUTE, were evaluated for their ab..ity to intain optimum damping capacity with time when stored at room temperature and 100°C, which represents a mperature range within which marine equipment commonly operate. Damping measurements were obtained using the dified resonant dwell technique. Significant degradation occurs within 12 days in both alloys when stored at om temperature or 100°C, although SONOSTON stored at 100°C exhibited stable damping in the active strain nge. Recovery treatments at 125°C indicated that a recovery mechanism was operative in INCRAMUTE, but absent SONOSTON. In fact a 125°C recovery treatment actually appeared to degrade damping in the active strain range SONOSTON. X-ray diffraction results indicated that the changing damping characteristics were unrelated to ttice changes detectable by that technique. Transmission electron microscopy revealed an unique contour umping" phenomena with electron beam heating, which is hypothesized to indicate a sensitive elastic ansformation, with a low strain threshold, of the tweed microstructure. In addition, although not antitatively evaluated, a modulus dicontinuity with time was observed upon initially vibrating cantilevers am specimens, possibly related to the necessity to activate the damping mechanism of the tweed microstructure.

DISTRIBUTION/AVAILABILITY OF ABSTRACT	21 ABSTRACT SECURITY CLASSIFICATION
☒ UNCLASSIFIED/UNLIMITED ☐ SAME AS RPT ☐ DTIC USERS	UNCLASSIFIED

NAME OF RESPONSIBLE INDIVIDUAL	22b TELEPHONE (Include Area Code)	22c OFFICE SYMBOL
L.J. PERKINS	2216	69Ps

FORM 1473, 84 MAR 83 APR edition may be used until exhausted
All other editions are obsolete

SECURITY CLASSIFICATION OF THIS PAGE

Approved for public release;
distribution is unlimited.

Damping Degradation in INCRAMUTE and SONOSTON Due to Low Temperature Storage

by

Lewis William Leary
Lieutenant, United States Navy
B.S., Georgia State University, 1979

Submitted in partial fulfillment of the
requirements for the degree of

MASTER OF SCIENCE IN ENGINEERING SCIENCE

from the

NAVAL POSTGRADUATE SCHOOL
December 1986

A B S T R A C T

Two commercial manganese-copper based alloys, SONOSTON and INCRAMUTE, were evaluated for their ability to maintain optimum damping capacity with time when stored at room temperature and 100°C, which represents a temperature range within which marine equipment commonly operate. Damping measurements were obtained using the modified resonant dwell technique. Significant degradation occurs within 12 days in both alloys when stored at room temperature or 100°C, although SONOSTON stored at 100°C exhibited stable damping in the active strain range. Recovery treatments at 125°C indicated that a recovery mechanism was operative in INCRAMUTE, but absent in SONOSTON. In fact a 125°C recovery treatment actually appeared to degrade damping in the active strain range in SONOSTON. X-ray diffraction results indicated that the changing damping characteristics were unrelated to lattice changes detectable by that technique. Transmission electron microscopy revealed an unique contour "jumping" phenomena with electron beam heating, which is hypothesized to indicate a sensitive elastic transformation, with a low strain threshold, of the tweed microstructure. In addition, although not quantitatively evaluated, a modulus dicontinuity with time was observed upon initially vibrating cantilevers beam specimens, possibly related to the necessity to activate the damping mechanism of the tweed microstructure.

TABLE OF CONTENTS

I. INTRODUCTION

A. GENERAL

It is common knowledge that all materials, metallic or otherwise, exhibit an ability to dampen propagating sound or any other form of applied force. However, certain alloys exhibit significantly higher inherent damping than others. Typically, these "quiet metal" alloys can be optimally heat treated to provide an even higher level of damping capacity. Unfortunately, in certain of these alloys, there is evidence that at ordinary storage or operating temperatures a metal component heat treated for a high damping capacity may experience a degradation in this capacity with time. This degradation of a alloy's damping capacity is of considerable interest since the development of high damping alloys would benefit the Navy by:

- reducing the low frequency acoustic emissions of both surface and submerged naval vessels, thus providing a tactical advantage;
- improving fatigue life, and thus service life, of equipment and machinery;
- reducing the hearing loss hazard to operating crews which occurs due to the ambient background noise common in machinery compartments.

Since damping degradation appears to be an aging phenomenon considerable attention has been directed at microstructural changes. In the high damping Mn-Cu alloys two characteristic microstructures, microtwins and tweed, have received considerable attention. It has been established for some time that the twinned sort of microstructure

provides a potent damping mechanism. However the capability of the tweed type microstructure is not completely characterized, and its damping mechanism is unknown.

B. DAMPING THEORY

Damping has a stress dependence [Ref. 1:p.129]. The general vibrational differential equation is,

$$my'' + cy' + ky = F \qquad \text{(eqn 1.1)}$$

where:

- m = mass
- c = viscous damping coefficent
- k = spring constant
- F = a time dependent forcing function
- y = displacement (y' and y'' are derivatives)

The viscous damping coefficent used above can be represented as:

$$c = 2m\zeta\omega_n \qquad \text{(eqn 1.2)}$$

where:

- ζ = a damping factor which varies between 0 and 1 (no damping = 0)
- ω_n = the natural angular frequency of oscillation

the steady state solution to Equation 1.1 is [Ref.1:p. 130]:

$$y = Y e^{i(\omega t - \varphi)} = F e^{i\omega t} / [(k - m\omega^2) + i\omega c] \quad \text{(eqn 1.3)}$$

where:

φ = the phase angle between the displacement response and the inputted excitation of the forcing function,

y = the displacement response,

Y = the displacement amplitude

Fe^{iwt} = the forcing function

w = the excitation frequency

A material's damping capability can be described by several interrelated relationships.

They are:

a. The frequency relationship - the difference between the frequencies of the half power points on both sides of the resonant frequency. This difference is normalized by dividing it by the resonant frequency [Ref. 2:p. 40].

b. The quality factor (Q) - the inverse of the frequency relationship [Ref 1:p.137]:

$$Q = w_n/(w_2 - w_1) \quad \text{(eqn. 1.4)}$$

c. Internal friction - (Q^{-1}), the inverse of Equation 1.4 [Ref. 2:p.41].

d. The specific damping capacity (SDC) - used empirically for a freely decaying oscillating system, i.e. a system without a forcing function. This relationship describes the decrease in the squares of adjacent stress amplitude peaks normalized by the square of the first amplitude [Ref 3:p.444]:

$$SDC = (a_{i+1}^2 - a_i^2)/a_i^2 \quad \text{(eqn. 1.5)}$$

SDC can also be defined as a ratio of the energy loss per cycle to the peak potential energy[Ref.4:p.70]. Equation 1.5 can be approximated, if the difference of the amplitudes are small, by [Ref. 3:p.444]:

$$SDC = 2(a_{l+1} - a_l)/a_l \qquad \text{(eqn. 1.6)}$$

There is also a relationship between the SDC and the normalized bandwidth of Equation 1.4, the quality factor, provided the damping factor << 0.5, [Ref.5:p.320]:

$$SDC(\%) = 200\ \pi\ Q^{-1} \qquad \text{(eqn. 1.7)}$$

e. Phase angle α or loss angle γ. The phase angle is the angle by which the strain lags behind the stress while under cyclic loading [Ref.3:p.445]:

$$\tan \alpha = \delta / \pi = Q^{-1} = 2\zeta \qquad \text{(eqn. 1.8)}$$

It can also be defined as the loss angle such that [Ref 1:p.137]:

$$\alpha = \tan \gamma = E^i/E^r \qquad \text{(eqn. 1.9)}$$

where:

E^i = dissipation modulus

E^r = real elastic modulus

tan c = loss tangent

f. The damping factor - as described in Equation 1.2 can also be used to describe damping.

g. The logarithmic decrement (δ) - for cyclic exponential free decay [Ref.1:p.138]:

$$\delta = \ln(a_l/a_{l+1}) = (1/n)\ln(a_o/a_n) \qquad \text{(eqn. 1.10)}$$

h. The amplitude dependence of the damping capacity in free decay for alloys aged to give high damping capacity is:

$$SDC = KA^n, \qquad \text{(eqn. 1.11)}$$

where: K = constant
A = strain amplitude
n = constant, dependent on the axial ratio

Equation 1.11 gives a linear log-log plot up to some limiting value of strain which depends upon alloy composition and heat treatment[Ref.6].

C. MACROSTRUCTURAL VIBRATION TECHNIQUES

Cu-Mn alloys, especially with a Mn content greater than 60%, have been widely studied using the Ke torsion pendulum device. The best description of this device's operation can be found in reference 4. Flexural free decay [Ref. 5] and longitudinal stress wave propagation along a rod [Ref.7] have also been used to determine damping in these alloys.

The research described in this paper was performed using the resonant dwell method, which utilizes an electromagnetic shaker to drive a cantilever specimen. Usually an optical microscope is mounted near the unclamped end of the cantilever to measure the free end's vertical displacement. This apparatus was modified by Professor Y.S. Shin by replacing the

optical microscope with acelerometers mounted on the cantilever tip and the clamped end (called the root). The signals from these acelerometers are compared and processed by a spectrum analyzer to produce the frequency response of the cantilever. This apparatus describes damping using a forced and continous vibrational input, instead of the free decay method common in the previously mentioned techniques. This has two advantages:

a. Provides a determination of the strain dependence of the damping exhibited.

b. Simulates the more realistic conditions of operating machinery experiencing operational stresses.

It is important to note that the traditional free decay method of testing may generate different results then the forced input methods discussed above. This is due to the fact that different damping mechanisms may be activated with these two kinds of testing systems.

D. METALLURGY OF THE MANGANESE-COPPER ALLOYS

1. Physical Properties

The Manganese-Copper alloy system includes an extensive single-phase FCC gamma solid phase miscibility of Mn in Cu at temperatures above 700°C [Ref.8], as seen in the phase diagram, Figure 1. Water quenching to room temperature from this FCC solid solution tends to retain this gamma phase. However, a miscibility gap exists in the Mn-rich portion of the Mn-Cu phase diagram between approximately 36 and 87 w/o Mn in a temperature range from 427°C to 600°C (the maximum occurs at 60 w/o Mn)[Ref.9]. This miscibility gap is sketched on Figure 1. The Neel and M_s temperatures become higher after

an alloy is conditioned by aging within this region of the phase diagram. Upon quenching to room temperature after such conditioning (at least for short aging times) a fine strain and/or compositional modulation (the "tweed") is generated. At longer aging times, a more distinct transformation to a face-centered tetragonal lattice cell may occur and an antiferromagnetic ordering is observed in the resulting martensite. The commercial high damping alloy INCRAMUTE has a composition which probably falls just outside this miscibility gap, while SONOSTON is clearly within the region.

2. Damping properties of Mn-Cu alloys

Several different damping mechanisms may operate simultaneously in Cu-Mn alloys. At low strain, normal relaxation mechanisms predominate; damping is independent of stress amplitude and varies with temperature and frequency. The damping from these mechanisms is, in general, insufficent to provide significant reduction in noise or vibration amplitudes. At high strains, the damping capacity is strain dependent; it is relatively frequency independent and to some degree temperature dependent. These mechanisms usually involve extensive generation and movement of dislocations, and strain hardening and fatigue damage is commonly experienced at these high strain levels.

The well known high damping capacity of certain Mn-Cu-based alloys has been commonly considered to be due to the presence and frictional activity of microtwins in a tetragonal martensite [Refs. 6,10,13:pp. 43,137,2104]. This mechanism is expected to be quite strain dependent. Tetragonal microstructures are absent in as-quenched Mn-Cu alloys with less 50 a/o Mn content [Ref.11:p.109], so that such compositions do not

possess a high damping capacity in the as-quenched condition. The highest damping is found in as-quenched alloys with greater than 82 a/o Mn.

For alloys which do not spontaneously become tetragonal on quenching, aging in the miscibility gap is required. For alloys conditioned in this way it is observed that the damping capacity increases with aging time, approaches a maximum value, and then declines as ageing continues. High damping capacity values are associated with the presence of a tetragonal structure, with the actual value of damping dependent on the composition, degree of lattice distortion (generated via the aging temperature, and the aging time), and temperature of observation [Ref.6]. The tetragonal phase is "ferroelastic" i.e., a reversible orientation of the tetragonal structure occurs easily, suggesting that quenched Mn rich Mn-Cu alloys should exhibit a shape memory effect [Ref. 12]. Alloys with high Mn content exhibit the greatest tetragonality [Ref.10:pp.132-133].

High damping capacity is thus considered to be manifested via the reversible, strain induced reorientation of the tetragonal domains due to migration of the microtwin boundaries [Ref.6]. The FCC -> FCT transformation induced by ageing the quenched alloys results in the formation of variously oriented small regions (microtwins) differing in the orientation of their tetragonal c-axis, twinned on {110} to maintain the overall form.

Thus the damping capacity of alloys of less than 82 a/o Mn concentration can be improved with aging. This is a consequence of the decomposition of the FCC gamma phase in the miscibility gap. Upon water quenching to room temperature the necessary tetragonality is created. The effect of aging time on damping is analogous to it's effect on other mechanical properties, that is, it increases with aging time to a peak then

decreases with overaging. This decrease with overaging is due to the creation of a high microtwin density which restricts the necessary boundary mobility.

The FCC -> FCT transformation differs from a normal martensitic transformation in that at high temperatures the stable cubic structure is continuous with the less symmetrical tetragonal structure and represents the special case of an axial ratio (c/a) of unity. Therefore, above the transformation temperature the damping remains low [Ref.6], and the operating or test temperature must be below the Neel temperature for damping to occur [Refs.6,10].

The a-parameter decreases monotonically with increasing temperature; the c-parameter increases with increasing temperature, at first slowly and then abruptly near the transformation temperature [Ref.12]. After the FCT -> FCC transformation, the a-parameter increases only slightly with temperature [Ref.12].

The effect of ageing (at 425° C of solution quenched alloys containing 60-90 wt./% Mn) is:

(1) to produce an overall contraction of the cubic lattice. The a parameter increases and the c parameter decreases respectively as Mn content increases, i.e., the axial ratio decreases gradually with Mn content [Ref.12]

(2) to progressively reduce the limiting Mn content required in the material to confer tetragonality at room temperature [Ref. 6].

Cell volume decreases with aging, with no discontinuity at the inception of tetragonality. Therefore, the FCC -> FCT transformation does not produce a change in cell volume and would not be influenced by the isostatic component of any applied stress [Ref. 6].

Tetragonal distortion increases the relative separation of the parallel to antiparallel magnetic moments between the twins [Ref.13]. This direction of contraction varies from region to region. Tetragonality and damping capacity begin to rise as the degree of magnetic order increases. The onset of this magnetic ordering is responsible for the martensite transformation, and the c/a ratio is a measure of the degree of order.

In the early stages of ageing there is an initial reduction in the rigidity modulus, followed by an increase as tetragonally increases [Ref. 6]. The transition temperature and the degree of tetragonal distortion increase as ageing proceeds. Alloys containing about 90 a/o Mn appear to be highly twinned on {101} planes after quenching from the gamma-phase field. Quenched alloys with over 82 at/% Mn are tetragonal at room temperature. Alloys containing less than 82 at/% Mn become tetragonal only when cooled to lower temperatures (such as at Liq. Nitrogen). [Ref.12]

Ageing also causes a change in the electrical resistivity. The time dependence of the variation in resistivity (for 70 wt./% Mn alloy) is of the form:

$$(R_t - R_{infinity}) = R_o e^{(-t/T)}$$

where: R_t = resistance after time t

$R_{infinity}$ = limiting value of resistance

R_o = initial resistance

t = time of ageing

T = time constant

The proportional change in resistance $R_{infinity}/R_o$ was the same throughout the range 400-475^{o}C. This indicates that the fully developed ordered structure is independent of temperature in this range [Ref. 6].

Birchon, Bromley and Hedley [Ref. 6] in 1968 suggested that the ageing process could be presumably controlled by interactions between Mn atoms. The overlap of orbitals of Mn ions results in a distortion of the lattice (with a critical separation of about 2.642 Angstroms). These interactions are enhanced by short-range diffusion during ageing; this results in "clustering," or a preference of Mn for certain crystallographic sites. This interaction depends upon the product of the concentration and the probability that a given Mn atom will have other Mn atoms as near neighbors. In a random arrangement this probability also varies with concentration, therefore the total interaction varies as the square of the concentration. In an ordered arrangement this probability is unity, thus the total interaction is directly proportional to the concentration. Thus in some compositions the effect of aging is to produce an ordered structure, the tweed [Ref. 6].

For energy to be dissipated, it may be necessary that the domain boundaries should be able to move against an impeding mechanism. Various possible means of impediment include:

(1) interaction with a-Mn precipitate particles

(2) interaction with features of a-Mn particle clusters (such as dislocation pile-ups, possible local magnetic changes, etc.)

(3) interactions with solute impurities.

Nittono, Satoh, and Koyama suggested in 1981 a mechanism for the tetragonal transformation in Mn-Cu alloys that parallels a similar transformation in the In-Tl alloys: The presence of a soft acoustic mode along <110> with a related <1$\underline{1}$0> polarized mode [Ref. 12]. The FCC -> FCT transformation results from this lattice mode softening. The "double shear process" is considered to be a coupling of 2 phonon modes (1 phonon mode = 1 shear movement of atoms). For example:

2 phonons: {g=0[110], e//[1$\underline{1}$0]} + {g=0[011], e//[0$\underline{1}$1]} corresponds to a shear:

(110)[1$\underline{1}$0]2e + (011)[0$\underline{1}$1]2e, where 2e=the shear angle.

The lattice correspondence between FCT and FCC is represented:

$$(1,1,1)_{fcc} \rightarrow (1+e,1-2e,1+e)_{fct}$$

The resultant axial ratio is (1-2e)/(1+e), which is less then unity. Neither the main domains or subdomains are defined in this hypothesis, but the domain interface is given as a boundary between the two variants which are to be transformed. The shear angle between 2 adjacent domains decreases continuously and reversibly, with increasing temperature becoming zero at the transformation temperature.

After ageing a mottled tweed-like structure appears under EM. This has been interpreted as being due to Mn- or Cu-rich areas formed before the precipitation of the equilibrium alpha-Mn (abrev.-aM) phase. The tweed structure was noted by Vitek and Warlimont to coarsen with increasing aging times [Ref.14].

Compositional changes due to aging occur and appear to be caused by:

(1) The formation of Cu rich regions; size=100 Angstroms. This is expected to occur at low aging temperature or short aging times. These regions are more prevalent in lower Mn content alloys [Ref.13].

(2) The precipitation of a-Mn. This is expected at high aging temperatures or long aging times. The nucleation of a-Mn should be favorable in the Mn-rich areas and this should result in a decrease in the Mn concentration of the matrix and the return to FCC [Ref.13].

The range of aging temperatures which results in FCT at room temperature, the degree of tetragonality, and the aging temperature of maximum tetragonality, all increase with Mn content [Ref.13]. Aging leads to a rapid increase in tetragonality until peak damping is achieved [Ref.10]. At this time an a-Mn precipitate becomes visible both at the

boundaries and inside grains. This results in: (1) removal of an active damping region, (2) precipitates acting as possible barriers to the growth of other microtwins [Ref.10].

There is a considerable increase in hardness prior to aMn precipitation, and Nittono, et al., [Ref.12] proposed that this occurred because concentration inhomogeneities developed before a-Mn formation. They further suggested that an intermediate decomposition reaction occurs owing to the existence of the metastable miscibility gap in the 2 phase gamma+alpha Mn region [Ref. 14]. They gave the presence of tweed structure as evidence for the development of this 2 phase region. This structure, even in unannealed samples, is due to the beginning of phase separation encountered upon quenching the samples from the gamma-region through the miscibility gap. The coarsening of this structure is due to the coarsening of the 2 phase structure. The strength of the magnetic interaction may be a function of the size of the Mn-rich areas, and thus part of the Neel temperature variation upon annealing may also be due to the coarsening of the 2 phase structure[Ref.14]. The twin domain size is much larger then the tweed, and thus neighboring Mn-rich areas must be coupled magnetically, with a common c-axis, when forming the twin domains.

A variation in tetragonality occurs after 2 hrs. of aging. The aging sequence is characterized by the sharp appearance of tetragonality and a gradual return to the cubic form at higher aging temperatures [Ref.13]. Similar variation in tetragonality occurs by isothermal aging. e.g.: 70/30 alloy becomes FCT after 15 min at 425^{o}C, but reverts to FCC if aged longer then 100 hrs [Ref.13].

Cold rolling is noted to cause a rapid decrease in the damping capacity [Ref.12]. This is due to the generation of a greater dislocation density, which impedes the mobility of the microtwin boundaries. Considerable strain hardening occurs during the first cycle of loading/unloading, then the shape of the unloading curve becomes insensitive to follow-on applications of stress and a closed hysteresis loop becomes symmetrical about a straight line equivalent to the mean modulus. Thus for an asymmetrical loading condition, energy dissipation as stress increases would be dependent upon earlier strain history; however energy dissipation during unloading is not influenced by prior strain [Ref. 6]. Stress effects are exhibited in a typical S-shaped curve, where the SDC increases with stress up to a maximum value and then levels off or drops off [Refs.6,10].

3. A Discussion of Microtwins and Various Descriptive Models

a. General

Among structural, displacive (diffusionless) phase transformations there are two distinct classes:

(1) At the unit cell level there is intracellular ("shuffle") displacement of atoms, with little homogeneous lattice strain. Long range elastic stresses in this case are considered to be negligible. This intracell displacive transition spreads with the speed of propagation of the associated soft phonon. The shuffle is a second order transition with well defined critical values and an approprlate soft mode polarization is observed [Ref.15]. The shuffling shifts selected atoms within the lattice to form a static phonon wave. When the intrinsic strain of these phonon waves gets high enough it causes the lattice distortion, thus the first class is preliminary to the second.

(2) The second class occurs when there is a significant lattice distorting strain of the unit cell, and the accompanying intracell shuffle strains are considered secondary. Lattice distortive transitions are essentially reversible, diffusionless, characterized by precise parent product habit planes and relative unit cell orientations, and shape reversible changes [Ref.15]. The unit cell distortion which

accompanies the formation and growth of the new product phase in the parent phase induces large elastic strains as well as long range dimensional changes [Ref.15]. As a result:

(a) The total free energy of the system becomes a function of not only of the intrinsic free energies of the homogeneous parent and product but of the free energy of the system's macroscopic heterogeneity as well [Ref.15].

(b) In martensites the elastic component of the total free energy is lowered either by irreversible plastic flow or by the formation of a heterogeneous array of the product phases in different crystallographic orientations, i.e. parallel twin bands [Ref.15]. Within parallel domains (twins) the elastic strain fields of the domains are oriented counter to each other.

(c) Although macroscopically soft elastic behavior frequently accompanies the transition, the transition is first order and mode softening never takes place completely [Ref. 15].

(d) Precursor structures, microdomains, frequently precede the transition [Ref.15].

b. A Soliton Model

Barsch and Krumhansl in 1984 developed a soliton model to describe the movement of microtwin boundaries [Ref.15]. More specifically, the elastic soliton wave solution of their model described the moving boundary between 2 velocity dependent orthorhombically deformed variants of the cubic parent phase. This model assumed the usual linear temperature variation of the soft shear modulus. The strain kink of this soliton moves with an alternating velocity (+/- v) vector in the [1$\underline{1}$0] direction, however the particles move parallel to the twin boundaries in the [110] direction at the speed of +/- $(2)^{.5}e_2 v$ [Ref.15]. The soliton is a relationship between the singularities among the phonons of the lattice. In the static limit of v=0, the deformation becomes tetragonal with axes in the [100],[010] directions [Ref.15].

For $T<T_c$, the model predicted an unstable cubic phase. For $T<T_c$, static kink solutions exist only if the phonon dispersion has upward curvature at small k. This is

confirmed by neutron scattering experiments. Therefore the model can describe static domain walls if the phonon dispersion is upward. In summation, this soliton is perpendicular to the domain wall and, on either side of the domain wall, pushes atoms along(parallel) the wall in opposite directions. Thus the boundary moves in the direction of the soliton and the atoms shift back and forth perpendicular to the soliton at the velocity of the kink.

This model presented several features:

(1) The coherent correspondence was maintained across twin boundaries, because the distorted lattice allowed the boundary to be "wavy".

(2) No atoms were "lost".

(3) Artifacts thought to be required to form the boundary, such as "coherency dislocations", became unnecessary.

The limitations of this model are:

(1) The model is only relevant when the strain field energy is an important part of the total boundary energy.

(2) The model cannot account for the Peierls barrier pertaining to twin boundary motion.

(3) The model cannot account for the balance between the core energy and elastic energy.

These limitations are features of dislocations, i.e. the model doesn't account for dislocations or barrier friction, and are only presented to provide a more complete view of the model. Since dislocations are a source of microtwin nucleation, this model may not be good description of the movement of microtwins at nucleation temperatures.

c. Microtwins in Mn-Cu

High damping capacity in Mn-Cu alloys has been assumed to be due to the stress induced movement of the twin domain walls [Ref.14], with a Neel temperature (T_n) greater than the test temperature (T_t) being the necessary condition for high SDC. When an elastic compressive stress is applied, domains with their c-axis most nearly parallel to the axis of compression will be nucleated, or grow at the expense of domains less favorably oriented. When the stress is released the domains shrink back anelastically to their original position [Ref.13]. Ease of microtwin movement, as well as the number of microtwins per unit volume, was at maximum at the aging treatment corresponding to the highest damping capacity [Ref.10]. The existence of a domain structure, as explained earlier, only occurs in tetragonal alloys. The magnetic ordering increases with decreasing temperature and the FCC -> FCT transformation occurs at 125^{o}C [Ref.13]. For the structure to magnetically order at a definite T_n upon cooling , the Mn enriched regions must be continuous [Ref.13]. This is because the Mn atoms become antiferromagnetically ordered at T_n [Ref.13]. In quenched samples where $T_n < T_t$, high SDC occurs only after annealing, during which Mn-rich regions form and the T_n increases [Ref.13].

d. Microtwin Nucleation

Dislocations act as the nucleation sites for microtwins [Ref. 10]. The nucleation of domains at dislocations can be induced under the electron microscope by focusing the beam and increasing the beam current. The stress fields of adjacent dislocations are important in this process, and nucleation often occurs at dislocations in a pile-up [Ref.13]. The Burgers vector of the dislocations of nucleation must lie in both the slip

plane and the domain boundary planes. This only occurs when the slip plane and the domain intersect in a <110> direction, therefore only a/2<110> screw dislocations nucleate domains [Ref.13]. Although they are the site for the nucleation of the damping microstructure, dislocations themselves in a high enough density hinder damping [Ref. 10]. Another site of domain nucleation is at a-Mn precipitate interfaces [Ref.13].

e. Features of Microtwins

A summary of the features of this structure are:

(1) The spin direction in the antiferromagnetic state is parallel to the tetragonal c-axis.[Ref. 14] It is this spin direction and its associated antifer romagnetic interaction in Mn rich alloys which results in contraction along the c axis creating tetragonality [Ref.10]. As Cu ions have no magnetic spin it is assumed that it acts to dilute the magnetic structure [Ref.10].

(2) The c-axis changes by approximately 90 degrees across the twin domain boundary [Ref.14]. Thus these twin regions make a 45^{o} angle to the {110} boundary wall [Ref.10]. The difference in orientation across a domain boundary is small (1^{o}) [Ref.13].Domain boundaries usually occur in parallel pairs and when inclined to the T.E.M. foil surface show a characteristic fringe pattern [Ref.13].

(3) Twin domains can extend across grains [Ref.14].

(4) Twin domains were never seen to move in the electron beam.

(5) After relatively long annealing (10 hrs at 500^{o}C, in Mn-Cu) subdomain formation was observed within the large domains previously formed [Ref.14].

(6) Domains are separated by coherent {101} boundaries [Ref.13].

Butler and Kelly suggested that to minimize internal strains the matrix becomes self-accommodating by splitting up into domains [Ref.13]. It should also be noted that the

FCT -> FCC transformation in Mn-rich alloys is correlated with the disappearance of long range antiferromagnetic ordering [Ref.10].

f. Temperature relationship

As the difference, $(T_n - T_t)$, increases both the magnetic interactions between domains as well as the density of domain walls increases [Ref. 14]. The increase in antiferromagnetic spin-coupling leads to an increase in the frictional forces of the domain wall movement; thus there is an increase in SDC [Ref.14].

As this difference continues to increase, domain walls increasingly impeded each other until they are finally pinned. At this point SDC drops off.

As test temperature increases the maximum attainable SDC decreases. This is due to either or both of the following effects:

(1) As T_t approaches T_n, twin wall density decreases and interaction strength between the walls and the decomposition structure decreases [Ref.14].

(2) The continuously coarsening structure will exert an increasingly stronger friction force upon the wall movement as a function of annealing time [Ref.14].

g. Absorption Mechanisms of Microtwins

Absorption of vibrational energy may occur with several possibilities:

(1) If there is a heterogeneous frictional effect on a very small scale between boundary movement and structure, vibrational energy would be transformed to heat and the ease of movement would probably depend on the misorientation across the twin boundary [Ref.10].

(2) It may be possible that the damping is directly associated with the antiferromagnetic structure. As the twin boundary moves through the Mn rich zones, magnetic moment rotation in the magnetic field of the neighboring ions occurs, which results in energy absorption [Ref.10].

(3) If it is assumed that the damping capacity is derived from the moving microtwin boundary, then the energy absorbed will depend on the volume of material that the moving boundary transverses [Ref. 10]. This appears to be the most plausible possibility since considerable microtwin movement occurs under stress in samples providing high damping capacity.

4. A discussion of the tweed microstructure

Tweed structures often occur in the early stages of precipitation when the parent phase is cubic and the precipitates are tetragonal. They are of interest since they may have some relationship to a material's damping. Tweed occurs in many systems and all involve an alignment of the tetragonal precipitate along the [110] directions of the cubic parent phase as well as the presence of shear strains of $\langle 1\underline{1}0\rangle$, {110} type. It is believed that tweed arises from a natural tendency to minimize the elastic energy of the precipitate distribution [Ref. 16]. This occurs in many alloys that undergo a displacive phase transition upon cooling. These two points distinguish tweed from spinodal decomposition since the latter usually has an alignment along the [100] directions and is the product of a short range reconstructive (diffusional) phase transformation. The image contrast of the tweed and the associated diffuse diffraction streaks are due to transverse lattice distortions of the [110] shear mode in combination with lattice instability. [Ref.17]

The strain modulations called tweed appear in the transmission electron microscope as fine striations, typically of 3-6 nm periodicity, [Ref.18] lying parallel to the {110} traces of the parent cubic phases. The $\{110\}\langle 1\underline{1}0\rangle$ type strains are also described as transverse displacement waves with $\langle 110\rangle$ wave vector and a $\langle 1\underline{1}0\rangle$ polarization vector [Ref.18].

The interaction of such waves results in a loss of cubic symmetry which translates the parent phase towards a tetragonal symmetry as the transformation approaches. This behavior is concurrent to temperature dependent parent lattice softening, and generates the distinctive diffuse microstructure identifible as a dense array of incommensurate shear strains. Incommensurate fluctuations in strain are usually associated with displacive mechanisms and, in particular, a periodic modulation of shear strains has been found to be common to most alloy systems that undergo a martensitic transformation. [Ref.18]

a. Mechanisms of Alignment

There are at least 3 mechanisms which could give rise to a tweed structure [Ref. 16] during the early stages of precipitation that could explain the [110] orientation:

(1) Preferential formation of precipitates in an aligned configuration. This seems incompatible with the observed formation of the tweed under conditions of high super-saturation, when the nucleation sites would be expected to be most random.

(2) The preferential coarsening of some precipitates which form a tweed at the expense of others. This seems incompatible with the observation of tweed in cases where the precipitates are too small for resolution by transmission electron microscope.

(3) The configuration of the precipitates into tweed after formation, i.e. the tweed occurs through the reconfiguration of small precipitates which initially form in a nearly random configuration.

b. A Computer Model

Wen, Khatchaturyan, and Morris in 1981 used this last mechanism to develop a dramatic computer simulation of tweed based on a progressive reconfiguration of a distribution of small tetragonal precipitates embedded in a two dimensional cubic matrix [Ref. 16]. The driving force for this reconfiguration was the associated decrease in elastic energy. This was computed in a long wavelength approximation using an assumption that the difference in elastic constants between the precipitates and the matrix phase was negligible. A specific treatment of the kinetics of the reconfiguration was avoided by choosing the reconfiguration steps so as to maximize the decrease in elastic energy. If the continuous transformation of an tetragonal element within the cubic matrix occurred coherently within the matrix then the precipitate would be internally shape strained in its elastic equilibrium state and would induce elastic distortions in the surrounding matrix and in adjacent precipitate particles [Ref. 16]. Other assumptions of the simulation were:

(1) The precipitates are large enough to be assigned their macroscopic elastic constant (the long wavelength approximation).

(2) Net strains are sufficently small for linear elastic relationships.

(3) The interfacial energy of the precipitate particles was neglected.

(4) The precipitate particles were modeled individually or as an aggregate of elementary particles which were defined by the cells of a superlattice laid downed over the undistorted matrix.

(5) Precipitate distribution was considered macroscopically homogeneous in the sense that any macroscopic subvolume of the matrix was like any other. This allowed the detailed shape of the external boundary of the matrix to be ignored.

(6) The transformation strain was considered rectangular, with a diagonal 2x2 matrix.

The simulation system was found to rapidly evolve into a metastable state in which all allowed elementary steps required an increase in elastic energy. At low temperatures the evolving simulation became trapped in this metastate. At high temperature, this same simulation would eventually escape due to thermal fluctuations [Ref. 16]. This escape from the metastate was followed by a further spontaneous evolution, which passed through a sequence of metastates of decreasing energy and increasing order of a "tweed like" appearance. The system then rapidly ordered into single variant lines, (11), which in 3D is equivalent to (110). The model finally provided a striking visual correlation with the physical appearance of the tweed structure in materials.

Results from the simulation indicate that a fine tweed formation results from an attempt to minimize the elastic energy of an assemblage of tetragonal precipitates.

c. A Study of V_3Si

Onozuka, Ohnishi, and Hirabayashi [Ref. 17] in 1986 suggested a model for the tweed structure in V_3Si where 'Embryos' with tetragonal symmetry nucleated locally and randomly upon cooling and generated directional strain fields in a cubic matrix. They found that the lattice planes had a "wavy" distortion with the shear mode forming an array of inclined noncubic regions, which merged into coherent twins with the enhancement of the fluctuating amplitude of the tetragonal distortion. Or simply, the embryos created a lattice wave which is the source of tetragonal distortions. In their observations they noted that as temperature is lowered below Tm, a mottled striation pattern, which eventually evolved into twin lamellae, were observed to originate from the tweed.

d. The Modulated Lattice Relaxation Model

Yamada recently advanced a model that describes the premartensitic phase orientation along the (110) vector in TiNi (which undergoes a BCC to orthohexagonal martensitic transformation)[Ref. 19]. The "Modulated lattice relaxation model" was an attempt to explain the asymmetric satellite pattern generated in diffraction patterns on an electron microscope. This model suggests that there exists a 'dip' in phonon dispersion waves. Since incommensurate waves of any kind, with a uniform amplitude through a crystal, cannot produce asymmetric shifts, he suggested that the modulation wave is spatially localized by crystal defects. If the elastic properties of the BCC lattice are normal (i.e. missing the dip) but the lattice has a defect then the lattice will relax monotonically around the defect. But if the dip is present then the relaxation around the defect will no longer be monotonic, instead it will cause modulation of the soft mode which is the mode at the bottom of the dip. This causes the asymmetry.

The premartensite phase was described as a state where 'embryos' (clusters of a few atoms) are randomly distributed spatially within a matrix which has a dip in the transverse phonon dispersion. At high temperatures embryo defects are randomly induced in this matrix by thermal excitation. As temperature decreases the embryo lifespan extends and a modulated relaxation of the lattice develops about each embryo. As temperature decreases further, the lattice relaxation amplitudes become larger, and embryo interaction becomes stronger. Finally at a critical temperature all of the embryos become oriented into one direction, where upon there is a transition to the macroscopic martensitic phase. He determined that the size of a dressed embryo should be of the order

of 100 Angstrom. Modulated lattice relaxation gives rise to long range indirect interaction between embryos. This tends to orient neighboring embryos into the same direction along equivalent <110> directions.

The pre-existing embryo theory of martensitic transformation assumed that large embryos of the order of 1000 angstroms are formed at high temperatures and are triggered at or below the M_s temperature. However such large embryos have not been directly observed [Ref.20]. It is speculated that the growth of the amplitude of premartensitic fluctuations as well as atom shuffling occurs at a temperature a few degrees above M_s. This indicates that the embryos could be much smaller then predicted (thus explaining their unobservablity) [Ref.20].

e. Magnetoresistance Effect

Anomalous magnetoresistance is common in premartensitic materials, and anomalous magnetoresistance peaks could be related to short wavelength displacement waves and periodic shuffling, as a precursor to the martensite transformation, which introduces additional Brillouin zone boundaries, thus altering the energy of the conduction electrons, which give rise to second order galvanomagnetic effects, i.e. magnetoresistance.

These anomalies have been variously interpreted to indicate a premartensitic instability of the parent phase and to suggest a progessive shear and distortion which carry the parent phase through a succession of metastable states to the final martensitic structure [Ref.20].

f. Static Displacement Wave Model

Oshima, Sugiyama, and Fujita [Ref.21], working with the tetragonal transformation in Fe-Pd, found the tweed structure to be induced by a static displacement of atoms, d{011}/[01$\bar{1}$], associated with the formation of disc-shaped martensite nuclei on the {110} planes of the austenite. The tweed microstructure persistently remained in the FCT martensite in the early stage of the transformation, where the degree of tetragonality was small and the c-axis directions of the small FCT martensite variants were tilted against each other [Ref.21].

The FCC-FCT thermoelastic martensite transformation in Fe-Pd alloys occurs in the FCC austenite phase with no ordering reaction and it was not accompanied with any precipitation. Lattice softening occurred in a temperature range up to 100^{o}K above the Ms temperature, where a characteristic change in tweed contrast was observed [Ref.21]. It was concluded that the slightly distorted lattice was formed by the localized soft phonon mode as a precursor to the martensitic transformation [Ref.21].

The tweed contrast was observed as separated spherical or stick like strain field contrasts with a density which is highest in the vicinity of both surfaces than in the interior of the specimen [Ref.21]. It was also noted that the tweed contrast did not appear in the interior of the twins introduced by the FCT transformation. The nature of the tweed contrast, which is a distinct image only under the dynamic diffraction condition, is typical of a dispersion of very small regions of elastic strain such as surrounding the coherent precipitates in the precipitation alloys [Ref.21].

The static displacement giving rise to the contrast is induced by the shear component on the (101) plane. Thus,

(1) The contrast change is analysed by assuming that the static displacements are R=d{110}/<110> (where: d = a small fraction of the atomic distance).

(2) Such displacements are parallel to the slip direction in FCC structures.

Oshima et al.,They suggested that the tweed origin is due to the formation of interlacing regions of small distortions in the FCC austenite phase [Ref.21]. Since the contrast continuously changes to that of the internal structure of FCT martensite, such locally distorted regions in the FCC austenite phase could arise from tiny FCT nuclei in the center of each region preceding the transformation to martensite. The presence of such martensite nuclei in the austenite phase was confirmed by the presence of diffuse streaks in the diffraction pattern, and their size was estimated to be below 3 nm [Ref.21].

These martensite nuclei form on the {110} planes because between the FCC and FCT structures the interfacial strains between $(110)_{fcc}$ and $(101)_{fct}$ is one order of magnitude smaller then in other cases. FCT growth appears to be preferred on both (101) and (110), however the actual displacement direction is only on the {110} planes, since (101) is not parallel to the c-axis. This suggests that martensite nuclei are produced on the {101} planes by a shear to the <112> direction [Ref.21].

g. Effects on the Modulus

Many lattices which transform martensitically, exhibit an anomalously low value of $.5(C_{11} - C_{12})$ near the M_s temperature, corresponding to the (110)<110> shear. As a review, the expression $.5(C_{11} - C_{12})$ defines the shear modulus, C'; C_{11} = Young's modulus

(stress in direction 1, strain in direction 1), C_{12} = (stress in direction 1, strain in a perpendicular direction to the stress). In a crystalographically similar alloy system (Au-Cd) to Mn-Cu, the value of $.5(C_{11} - C_{12})$, as well as the M_s temperature, changed as the alloy composition changed. The mechanical instability of the beta phase with respect a (110)<110> shear can be viewed as a long wave length lattice displacement wave [Ref. 20].

Since the elastic constant, C', represents the resistance against the shear motion of <1$\underline{1}$0> direction on the {110} plane, the lattice instability in the {110}/<1$\underline{1}$0> shear mode can be assumed to be connected to FCT nuclei formation [Ref.21]. Such nuclei would be distributed to minimized the strain energy of the system.

h. Temperature Effects

The enhancement of the tweed contrast immediately before the Ms temperature indicates that this is the full growth stage of the pre-existing nuclei, which can be described by cooperative atomic movements affected by the interaction between small growing martensite platelets with different c-axis variant directions [Ref.21]. At the Ms temperature the transformation takes place by the coelescence and rearrangement of the nuclei. Also at this temperature, fine fringes lying along the {200} planes appear in areas where the enhanced striations cross each other [Ref.21]. This effect arises due to the difference of the interplanar spacings of 2 overlapping FCT regions possessing mutually perpendicular c-axes.

E. DAMPING DEGRADATION OR DAMPING INSTABILITY

"Damping degradation", "damping loss due to storage", and "damping instability" are expressions of the same phenomena. DAMPING STABILITY, or in brevity "stability", is

defined as: the ability of a material to retain its damping character with respect to time and storage temperature. "Instability" refers to the loss of this damping ability. A damping degradation phenomenon in INCRAMUTE, a Cu-Mn alloy, was reported in INCRA REPORT no. 274 in 1978 [Ref.22], which describes the behavior of two variations of INCRAMUTE. INCRAMUTE I experiences a reversible loss of damping above 65°C, and was modifed by adding tin to create INCRAMUTE II with a temperature limit of 125°C [Ref.22, p.1].

It was determined that there were two forms of damping loss. Reversible loss of damping begins at the damping transition temperature (DTT), which is itself dependent on the aging treatment, see Table 1.

TABLE 1. DAMPING TRANSITION TEMPERATURE IN INCRAMUTE

ALLOY	8HR AGED	24HR AGED
INCRAMUTE I	65°C	95°C
INCRAMUTE II	-	125°C

Irreversible loss of damping capacity occurs upon storage between room temperature and the damping transition temperature (DTT), and the mechanism by which this occurs is believed to operate above DTT as well.

The damping of INCRAMUTE was found to degrade when stored under no stress at temperatures below DTT, with the highest degradation in the range 20 - 50°C. Recovery of damping was reported [Ref.22] to be possible by heat treatment for a short period of time just above DDT (125°C for 30 min.). This effect is called RECOVERY.

The magnitude of instability as a function of time for storage under no stress appears to decrease as the solution treatment temperature used approaches the minimum recommended temperature for solid solution treatment (700°C for INCRUMUTE). Also cyclic stressing was reported to have "a strongly deleterious effect"[Ref. 22] on stability. It was implied that the effect of storage degradation is to also weaken the resistance of the damping stability to cyclic loading. No instability was observed when storage was under constant tensile stress.

The suggested mechanism for these damping effects was based on the mobility of the microtwin boundaries. The magnitude of the damping capacity is determined by the density and mobility of these boundaries. No damping occurs above DTT since the microtwins do not exist at these temperatures and thus cannot cause a damping effect. DTT is closely related to the ordering temperature, which is approximately the Ms temperature, at which these microstructures form. However, storage above DTT prevents instability of room temperature damping. Instability is reportedly caused by the continued development of subdomains during storage which lock existing domain boundaries. The effect of an applied static tensile stress is to inhibit subdomain development, thus damping stability is maintained. Under cyclic loading, accumulated substructural defects, such as dislocations, could hinder twin-domain motion, and thus

degrade damping stability. The phenomena of recovery is believed to result from the complete release of the locked domain structure as the tetragonal lattice distortion associated with the antiferromagnetic ordering is eliminated. Stability after recovery was not reported [Ref.22], but presumably the whole process of twin domain formation on cooling, sub-domain development on storage, etc., repeats itself.

INCRUMUTE aged at 400°C for 8 hrs, then stored at room temperature became unstable after 10 weeks, while INCRUMUTE I aged at 400°C for 24 hrs, then stored at room temperature became unstable after 3 weeks [Ref. 22]. This strongly indicates that the rate of instability is sensitive to prior heat treatment, in this instance increasing as aging time is increased.

Hardness readings and c/a ratio did not change during the storage degradation or following retransformation [Ref. 23]. This indicated that the damping capacity in INCRAMUTE is relatively insensitive to the degree of tetragonality [Ref.23].

Recovery of the domain mobility apparently occurs when subdomains are eliminated. The recovery treatment has an insignificant aging effect, and a-Mn is not precipitated at the low recovery temperature. Recovery allows the domain structure to be redistributed according to the dislocation arrangement that exists above the Ms temperature. However if the dislocation density is too high (greater than 10% plastic deformation) damping is low and cannot be recovered. [Ref.23]

II. EXPERIMENTAL PROCEDURE

The experimentation in the present wok was designed so that initially all specimens were at or near their highest damping capacity. Optimum damping in INCRAMUTE was found, in the previous research of Reskuvich, to require a 16 hour aging treatment at 400^{o}C [Ref.24], while SONOSTON's optimum damping treatment was unknown and had to be determined. Four specimens of SONOSTON were solution treated for 2 hours at 800^{o}C in evacuated VYCOR quartz tubing, then water quenched to room temperature. This was followed by an aging treatment in PYREX vacuum sealed tubing at 400^{o}C at four aging times (2,4,8,16 hours). These specimens were finally water quenched to room temperature. This process determined that the best damping treatment for SONOSTON at 400^{o}C was at the four hour aging time. The composition of the two alloys, INCRAMUTE and SONOSTON, is detailed in Table 2.

TABLE 2: ALLOY COMPOSITION

ALLOY	Cu	Mn	Al	Fe	Ni
INCRAMUTE	58	40	2	0	0
SONOSTON	37	54.25	4.25	3	1.5

All specimens, both INCRAMUTE and SONOSTON, were solution treated for 2 hours at 800°C in evacuated VYCOR quartz tubing, then water quenched to room temperature. The respective optimal damping aging treatments for the two alloys were then done in PYREX vacuum sealed tubing at 400°C, and the samples were finally water quenched to room temperature. These very similar heat treatments for the two alloys were conducted in order to provide a direct comparison of the compositional effects. To prevent unwanted aging at room temperature specimens were stored, when necessary, in a freezer at -22°C.

Two storage temperature conditions, at room temperature (19°C) and at 100°C, were evaluated. Five SONOSTON and four INCRAMUTE cantilever specimens were stored at each temperature. Initially the storage period was intended to be over a period of five weeks; however storage degradation proved to be more accelerated then expected, so that the storage period eventually was shortened to 12 days. The remaining specimens were then recovery treated at 125°C for 30 minutes to observe the phenomena of recovery. Including the 4 specimens needed to determine the optimum treatment for SONOSTON a total of 16 cantilever specimens were evaluated for damping.

Transmission electron microscopy was conducted on a JEOL JEM-100CX II electron microscope operating at 120kV. Foils of both alloys were prepared from 3 mm diameter discs having an average thickness of 0.02

inches. These discs were jet polished using a potential of 40 volts for 35 seconds in a solution of 50% H_3PO_4 in water. Static polishing to performation was then accomplished in a magnetically stirred saturated solution of 50% CrO_3 and 50% H_3PO_4 at 10-20 volts. The jet polishing tended to produce an undesirable preferential grain etching effect that had to be carefully avoided.

Lattice parameters were determined for the four conditions using the Philipps XRG-3100 X-ray diffractometer with a Copper tube (wavelength = 1.5405 Angstroms). The X-ray specimens were statically polished in a magnetically stirred saturated solution of 50% CrO_3 and 50% H_3PO_4 at 30 volts to relieved residual surface stresses induced by mechanical polishing.

Damping measurements were conducted at room temperature (approximately 19^{o}C), in air, using the modified resonant dwell technique of Reference 25. This apparatus compares the signals from two accelerometers using a Hewlitt-Packard HP-3582A Spectrum Analyzer to produce the transfer function frequency response for the vibrating cantilever. One accelerometer is placed on the clamped end, called the root, and the other is placed on the vibrating tip of the cantilever. Two modes were tested on each cantilever, with the exception of the preliminary SONOSTON tests which used 3 gages per cantilever. A strain gage at mode 1, at the root, measures the maximum strain and corresponds

to the natural frequency. An excellent discussion of the theory and calculations is provided in Reference 24 [p.37]. Resistive type foil strain gages (type CEA-13-250UN-350) were mounted at the longitudinal positions corresponding to the suprema of the maxima for the respective modes examined. The actual strain gage placement for the cantilevers of both alloys is shown in Figure 2 along with the cantilever dimensions. Background 60 Hz household source interference was experienced in both alloys during mode 1 excitation at low level loading. At higher loading conditions this effect disappeared. Furthermore, data for these affected low strain levels was provided by mode 2 strain gages, which were uneffected by this background electrical source.

Frequency data sampled from the root and tip accelerometers, for each mode, at various loading conditions, were averaged for 128 samples using the frequency spectrum analyzer. Using the half power method at resonance the SDC was determined from the frequency response curve for each mode under various loadings. A Wheatstone bridge amplified the resistive voltage generated by the attached foil strain gages. The HP-5451C Fourier Analyzer sampled this amplified strain voltage for five seconds and calculated, via the analyzer's algorithm, a value in V_{rms}^2. Peak strain was then calculated using the bridge conversion of 2000 qe/V.

III. RESULTS AND DISCUSSION

A. GENERAL DESCRIPTION OF SDC DATA

Various typical features of a SDC vs. strain semi-log plot are depicted in Figure 3. The strain at which SDC begins to exhibit significant strain dependence can be referred to as the activation strain. This strain value may be used to arbitrarily separate the nonactive low strain range from the high strain range where an active absorption mechanism is present. The activation strain indicates a critical strain above which a significantly more potent absorption mechanism becomes active.

The "nonactive SDC" refers to the average SDC in the nonactive low strain range, where the slope of the SDC-strain plot is effectively zero. The nonactive SDC value reflects damping sources which are either nonabsorptive and strain independent, or possessing an absorptive mechanism that functions at all strain levels. The peak SDC and peak strain (at peak SDC, of course) typically occur in the absorptive high strain range.

B. OPTIMUM DAMPING CONDITION OF SONOSTON

The optimum heat treatment for Damping Capacity in SONOSTON was determined to be a 4 hour aging treatment at 400°C, as shown in Figure 4. The optimum treatment for INCRAMUTE had been previously determined by Reskuvich to be a 16 hour aging treatment 400°C [Ref. 24].

C. DAMPING DEGRADATION OF INCRAMUTE

The damping loss in INCRAMUTE for storage temperatures of room temperature and 100°C, are depicted in Figures 5 and 6 respectively. The peak SDC, the peak strain, and the activation strain were all less then the values determined by Reskuvich using the same apparatus and method. The SDC over the nonactive strain range also appeared to decrease slightly.

D. DAMPING DEGRADATION OF SONOSTON

The damping loss in SONOSTON for storage temperatures of room temperature and 100°C, are depicted in Figures 7 and 8 respectively. When compared with the INCRAMUTE alloy, SONOSTON showed better damping stability in the absorptive range, while in the nonactive range a more dramatic SDC decrease is exhibited by SONOSTON than by INCRAMUTE, with the nonactive SDC of SONOSTON dropping from 17% to 9% after 12 days storage at 100°C. For this same storage treatment, the absorptive range appears to be unchanged, with the exception of the activation strain

which appears to have increased. Although it appears that the peak SDC has increased, the effect may be due to graph fitting. The apparent lack of degradation maybe due to either a more stability resilient aging treatment (i.e., slower degradation kinetics for the process in SONOSTON than in INCRAMUTE), or the SONOSTON specimens may have a damping transition temperature below 100°C. In the latter case, the absorptive mechanism would not have degraded since it would, at 100°C, be inactive. When the response is compared with that of INCRAMUTE, where the 100°C temperature did lead to high strain degradation, the explanation of a lower transition temperature in SONOSTON seems reasonable.

E. EFFECT OF A 125°C RECOVERY TREATMENT

The effects of a supposed "recovery" treatment at 125°C on SONOSTON (after degradation at storage temperatures of room temperature and 100°C, respectively) are shown in Figures 9 and 10. Similarly, Figures 11 and 12 show the damping "recovery" effect of the 125°C treatment on INCRAMUTE.

After a 125°C treatment for 30 minutes, room temperature stored SONOSTON appears to suffer a degradation of damping instead of a recovery, with the nonactive SDC dropping to as low as 4%. Also, 100°C-stored SONOSTON shows a decrease of damping capacity in the absorptive region after the 125°C treatment.

INCRAMUTE stored at room temperature and then treated at 125°C treat shows some recovery of damping, however the recovery is to a level substantially below the previous optimum level. On the other hand, a 125°C recovery treatment applied to the 100°C-stored INCRAMUTE produces a recovered level of damping which actually exceeds the original nonactive SDC by a multiple of two, and the strain-dependence becomes negative, i.e. SDC decreases from the nonactive to the active region. Rigorous attention has been given to assure that this curious result is a correct observation.

A general statement of these results is that INCRAMUTE exhibits a favorable recovery effect from a 30 minute, 125°C treatment, while SONOSTON fails to exhibit such an effect.

F. STRAIN ANOMALY ON INITIAL CYCLING

In the course of carrying out the routine of damping experimentation on these alloys, it was noted that there characteristically appeared to be a pronounced strain amplitude shift with time, as shown in Figure 13. When an untested cantilever beam was initially driven by the shaker, strain measurements, taken approximately every 30 sec, initially settled to a relatively low strain value, but after a short time interval (approximately 4-5 minutes), a discontinuous increase to a higher value was noted. Subjectively, even the visually apparent vibration amplitude of the cantilever beam could be noticed to change. It was thought at

first that this effect was perhaps due to some sort of experimental characteristic, such as in the circuitry of the strain gage being used. But later measurements on the same beam, made with other gages, did not show a repetition of this discontinuous strain effect. Combined with the visually apparent change in the vibration amplitude, this indicates that the strain in the sample is indeed affected with some time dependency. Since the inputed force of the shaker can be reasonably assumed to be constant, it must be hypothesized that under initial cyclic stressing the elastic modulus experiences a discontinuous decrease after a certain activation time. A more rigorous evaluation of this phenomenon is indicated.

G. TRANSMISSION ELECTRON MICROSCOPY RESULTS

Only a limited amount of electron microscopy was conducted, but the observations that were made seem to indicate the absence of the expected microtwinned microstructure in both alloys, and rather the presence of a tweed type microstructure. In SONOSTON a slightly modulated surface seems to indicate that a tweed may be present, but the distinctive tweed morphology reported by Reskuvich for INCRAMUTE (in the optimum heat treated condition) was not found. An interesting indication of the response of these structures to local stresses was provided by the observation of a dramatic jumping effect for bend contours under conditions of local electron beam heating, as evidenced by a spastic

shifting of the contour lines. The microstructural change, if any, that accompanies this behavior could not be noticed, but would seem to indicate some sort of very sensitive elastic transformation, and deserves further attention.

IV. CONCLUSIONS

The following conclusions are presented for this thesis:

(1) The problem of developing an optimum thermal treatment for the development and retention of useful high damping in an operational component of a Cu-Mn based alloy has not been completely solved. This problem is exacerbated by the conflicting aging times and aging temperatures required by each of the following damping attributes:

   (a) maximum damping,

   (b) best damping stability,

   (c) the desired transition temperature.

(2) The Mn-Cu based alloys INCRAMUTE and SONOSTON exhibit fairly rapid degradation of strain-active damping when stored at room temperature or 100°C.

(3) Degradation of damping due to low temperature storage, and recovery of damping due to subsequent heat treatment are different in INCRAMUTE and SONOSTON. This may be due to compositional, kinetic, microstructural or transition temperature differences.

(4) There appears to be a strain and modulus discontinuity soon after initiation of cyclic stressing, possibly corresponding to a time dependent process of activation of the strain-sensitive features in the microstructure.

(5) Furtherwork is indicated to solve the dilemma posed in point 1 above.

APPENDIX
FIGURES

PHASE DIAGRAM OF CU–MN SYSTEM

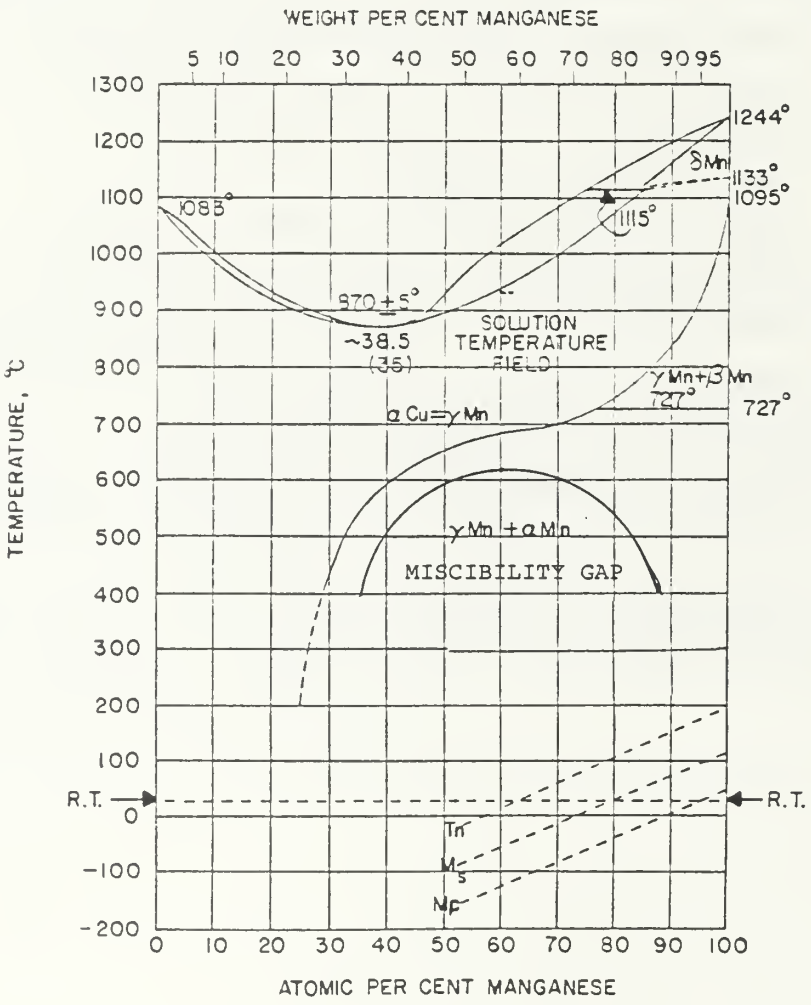

FIGURE 1.

CANTILEVER DIMENSIONS AND GAUGE PLACEMENT

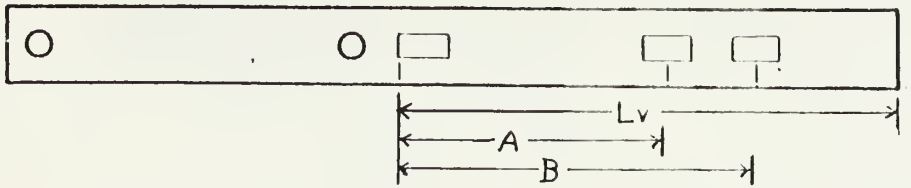

	SONOSTON	INCRANUTE
Overall length	8.50"	8.35"
Vibrating length (Lv)	5.00"	4.85"
2nd modal length (A)	2.65"	2.75"
3rd modal length (B)	3.55"	3.44"
Width	.50"	.50"

FIGURE 2.

TYPICAL SDC–STRAIN PLOT

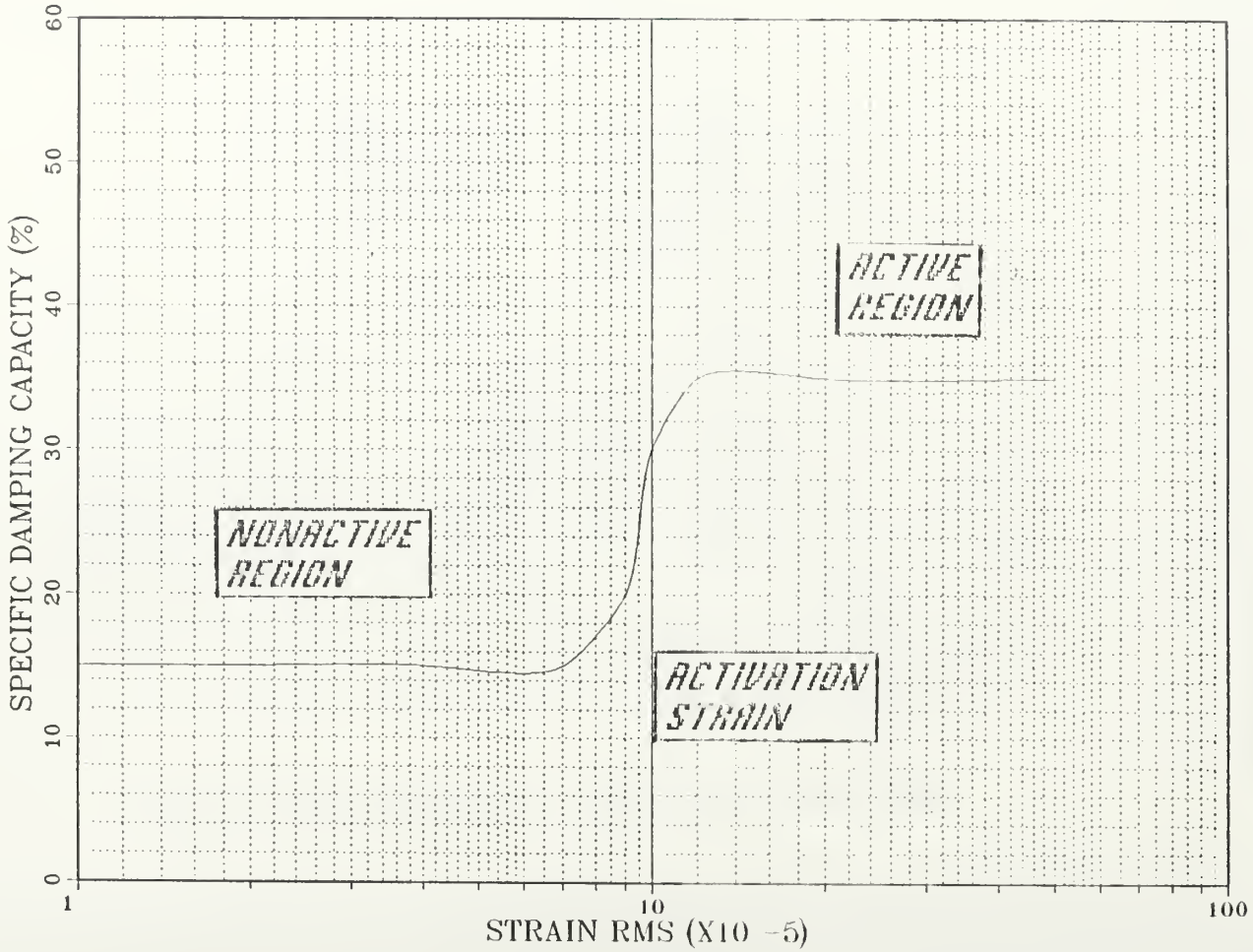

FIGURE 3.

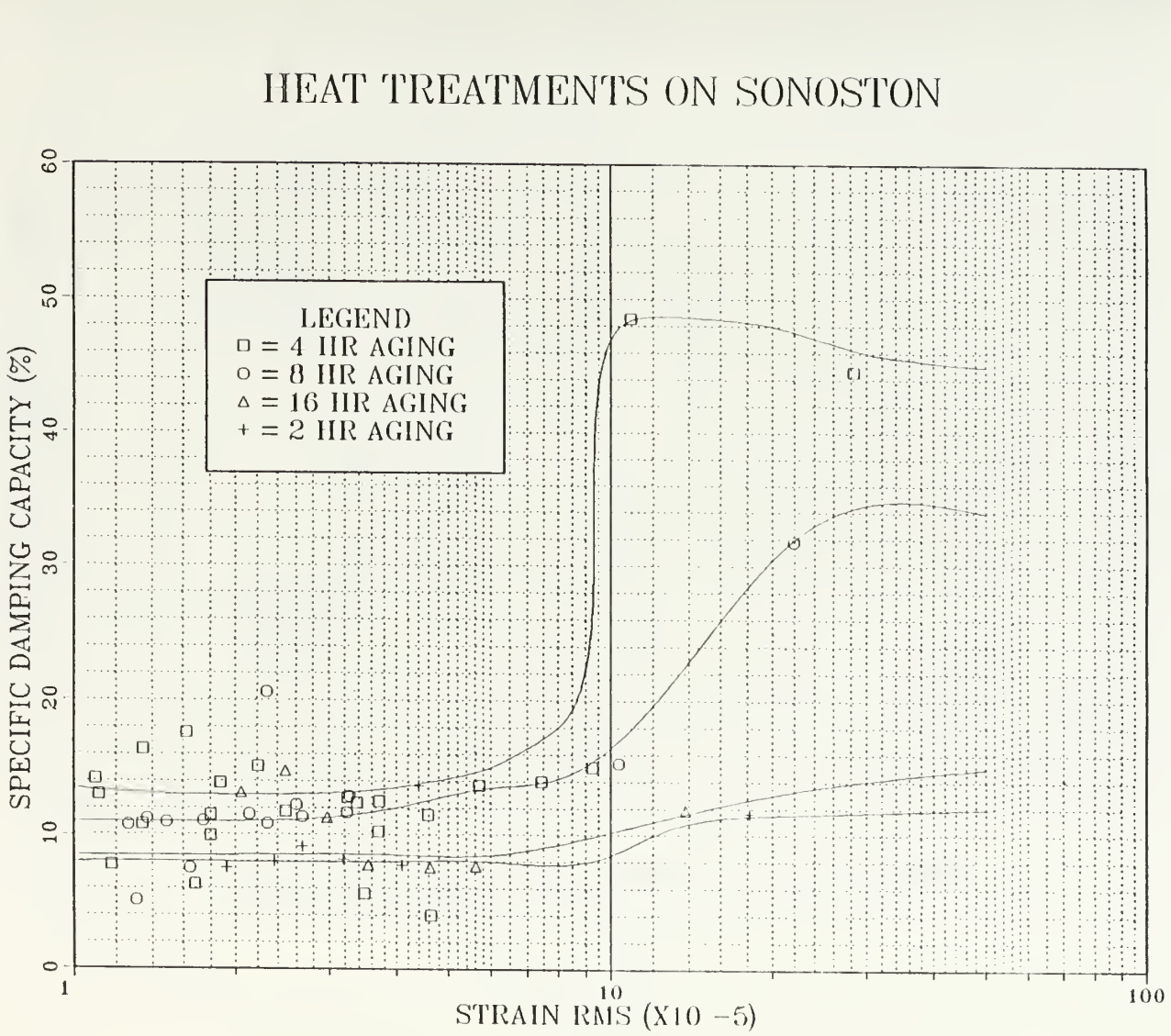
HEAT TREATMENTS ON SONOSTON
LEGEND
□ = 4 HR AGING
○ = 8 HR AGING
△ = 16 HR AGING
+ = 2 HR AGING
SPECIFIC DAMPING CAPACITY (%)
0
10
20
30
40
50
60
1
10
100
STRAIN RMS (X10 −5)

FIGURE 4.

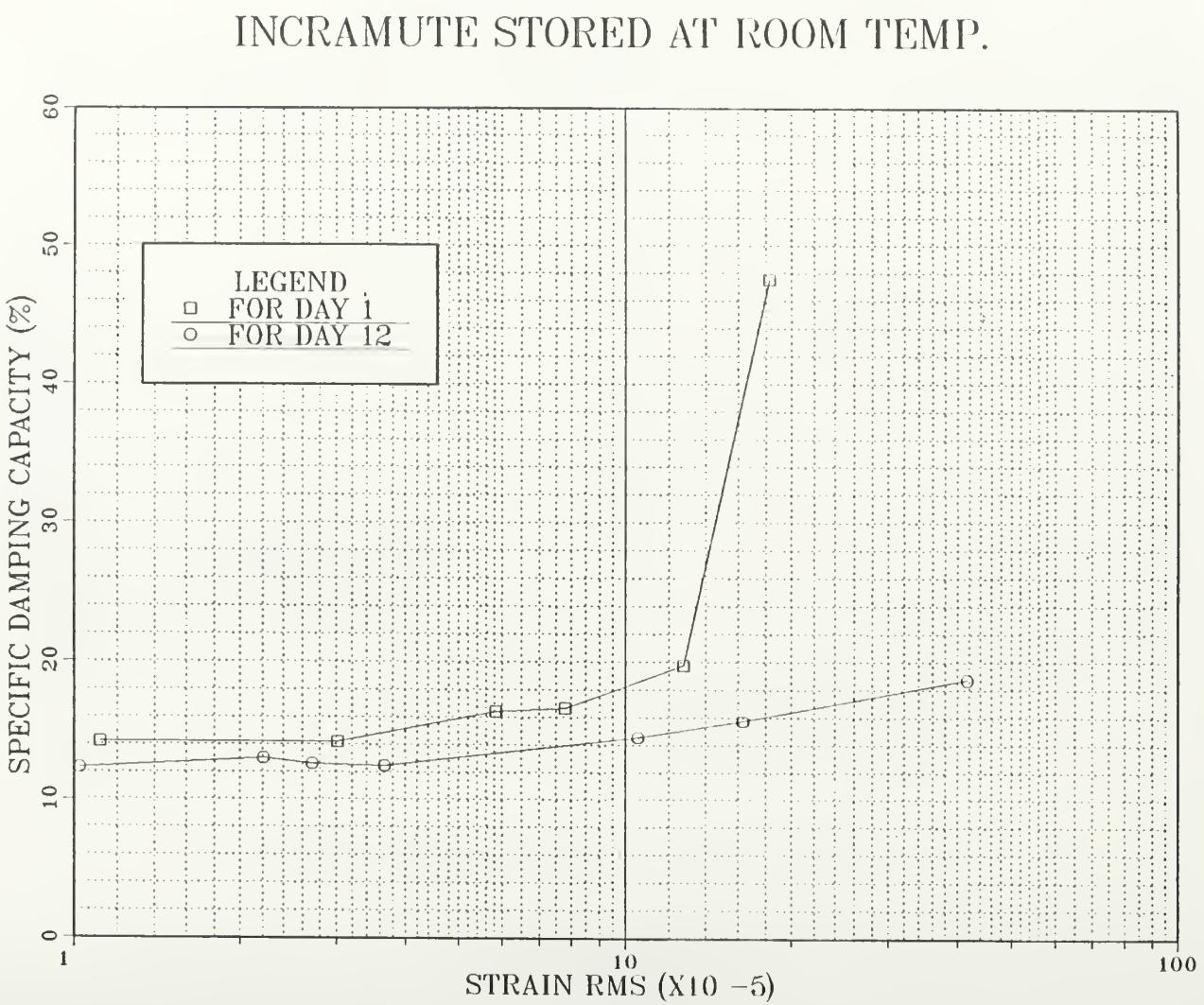
INCRAMUTE STORED AT ROOM TEMP.
LEGEND
FOR DAY 1
FOR DAY 12
SPECIFIC DAMPING CAPACITY (%)
0
10
20
30
40
50
60
1
10
100
STRAIN RMS (X10 −5)

FIGURE 5.

INCRAMUTE STORED AT 100C

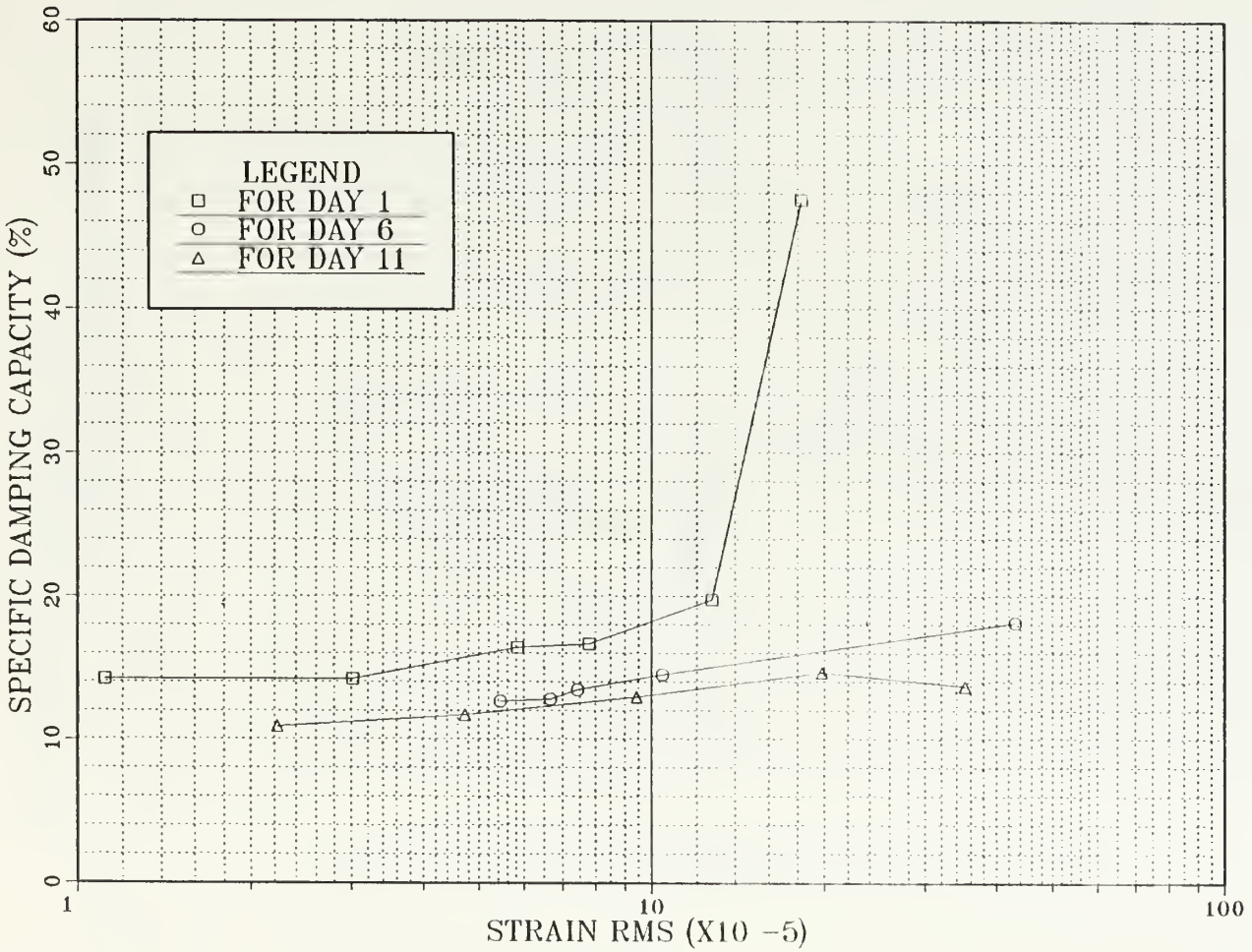

FIGURE 6.

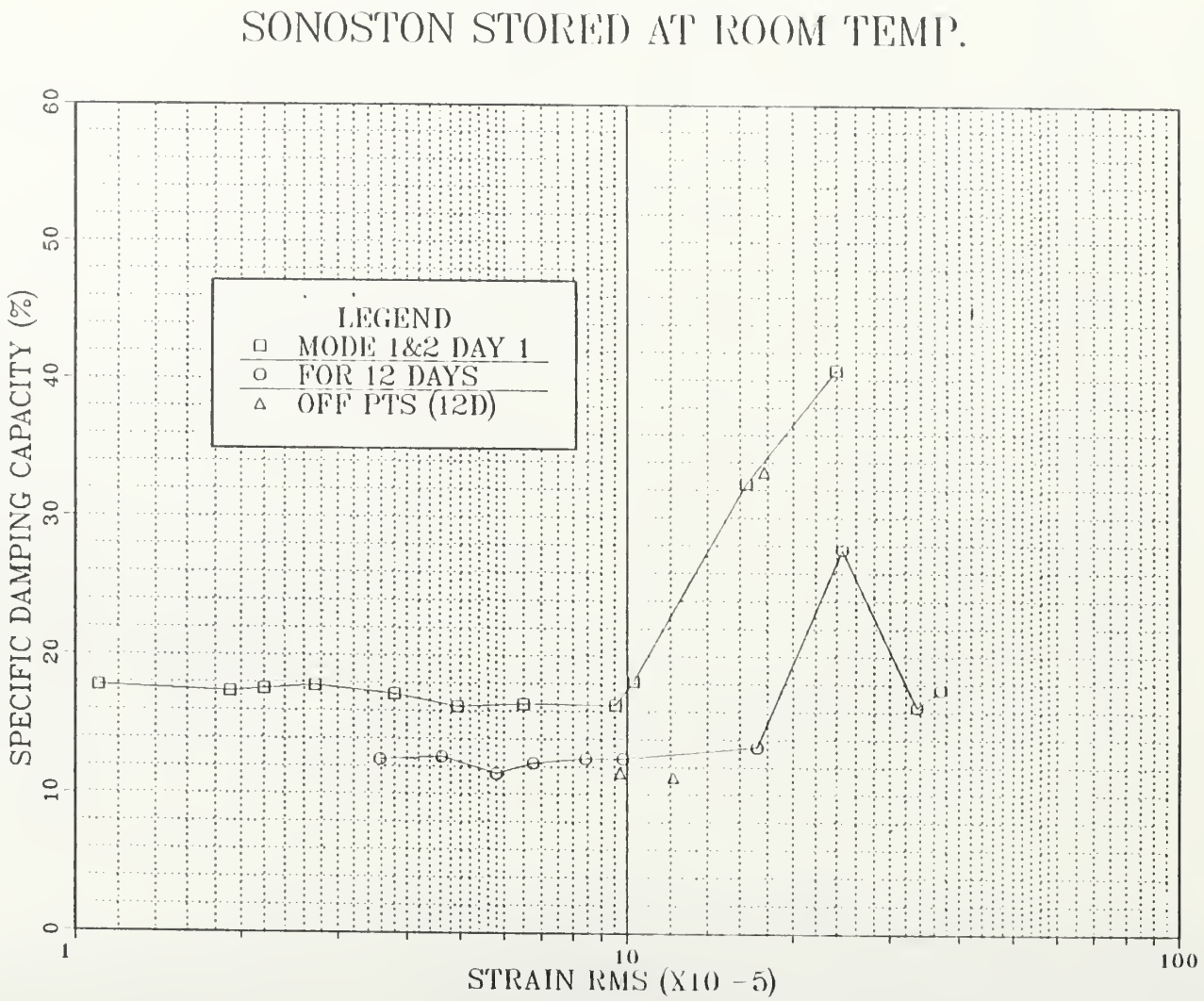
SONOSTON STORED AT ROOM TEMP.
SPECIFIC DAMPING CAPACITY (%)
0
10
20
30
40
50
60
LEGEND
MODE 1&2 DAY 1
FOR 12 DAYS
OFF PTS (12D)
1
10
100
STRAIN RMS (X10 -5)

FIGURE 7.

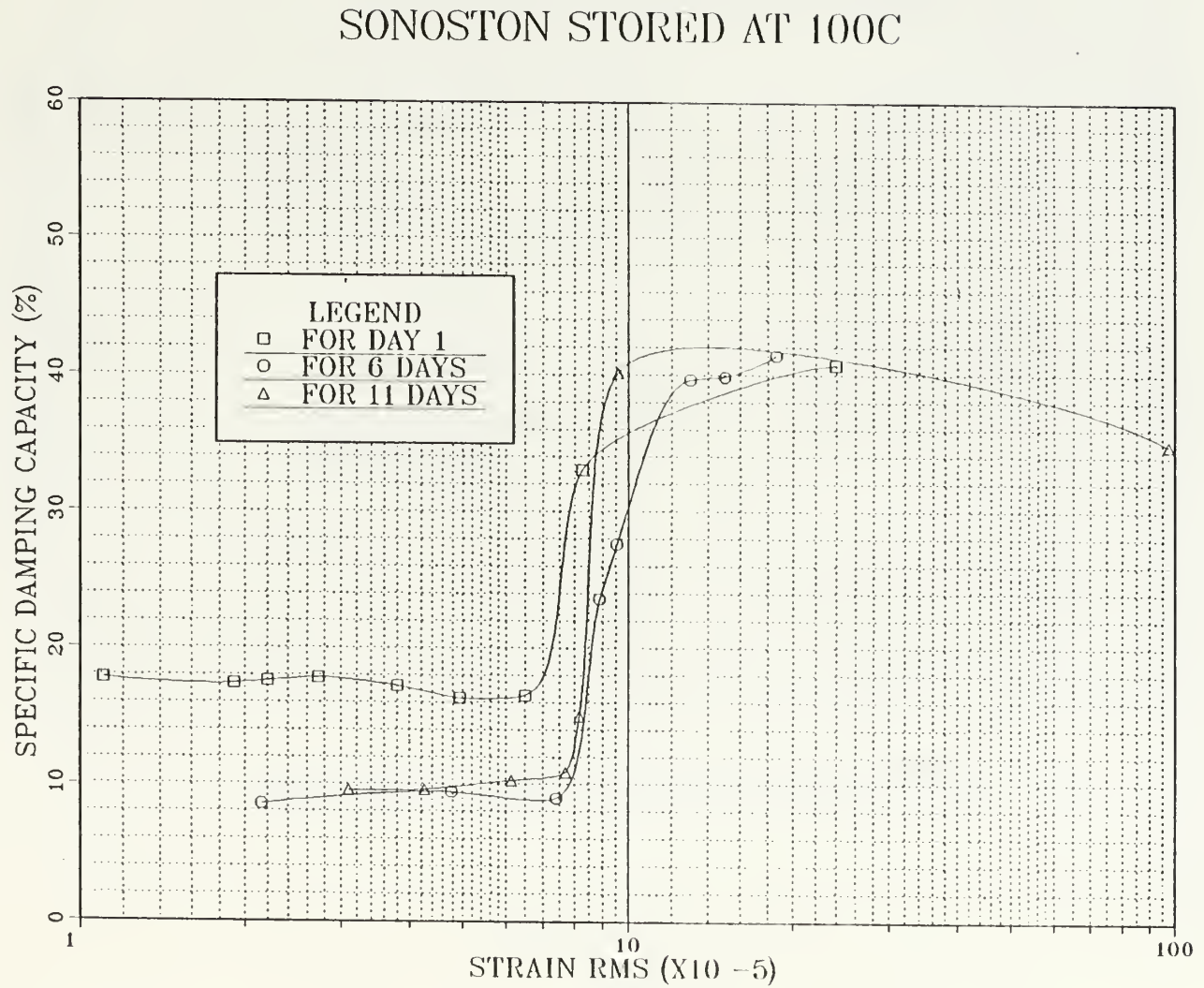
SONOSTON STORED AT 100C
SPECIFIC DAMPING CAPACITY (%)
0
10
20
30
40
50
60
LEGEND
FOR DAY 1
FOR 6 DAYS
FOR 11 DAYS
1
10
100
STRAIN RMS (X10 -5)

FIGURE 8.

SONOSTON RECOVERY (ROOM TEMP)

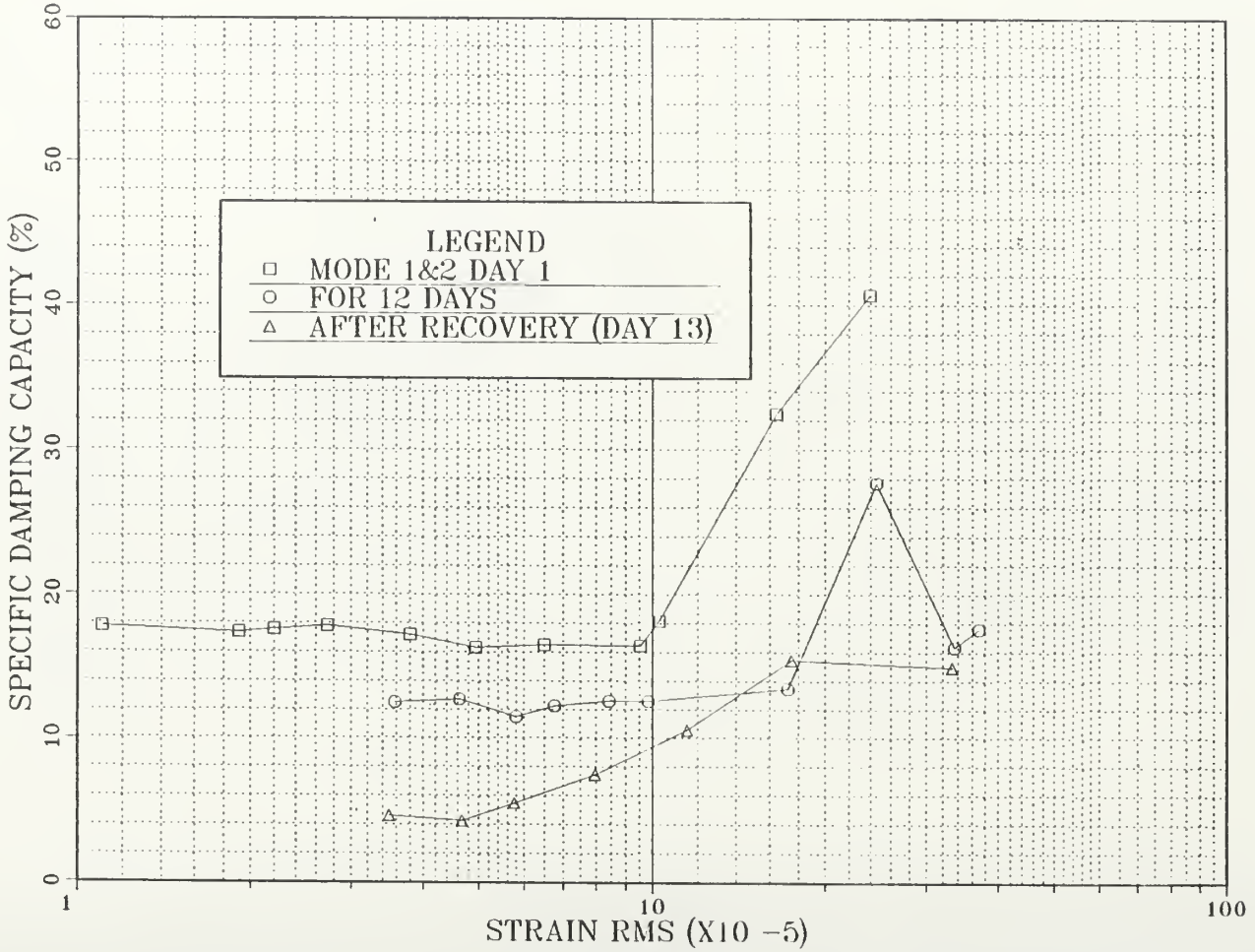

FIGURE 9

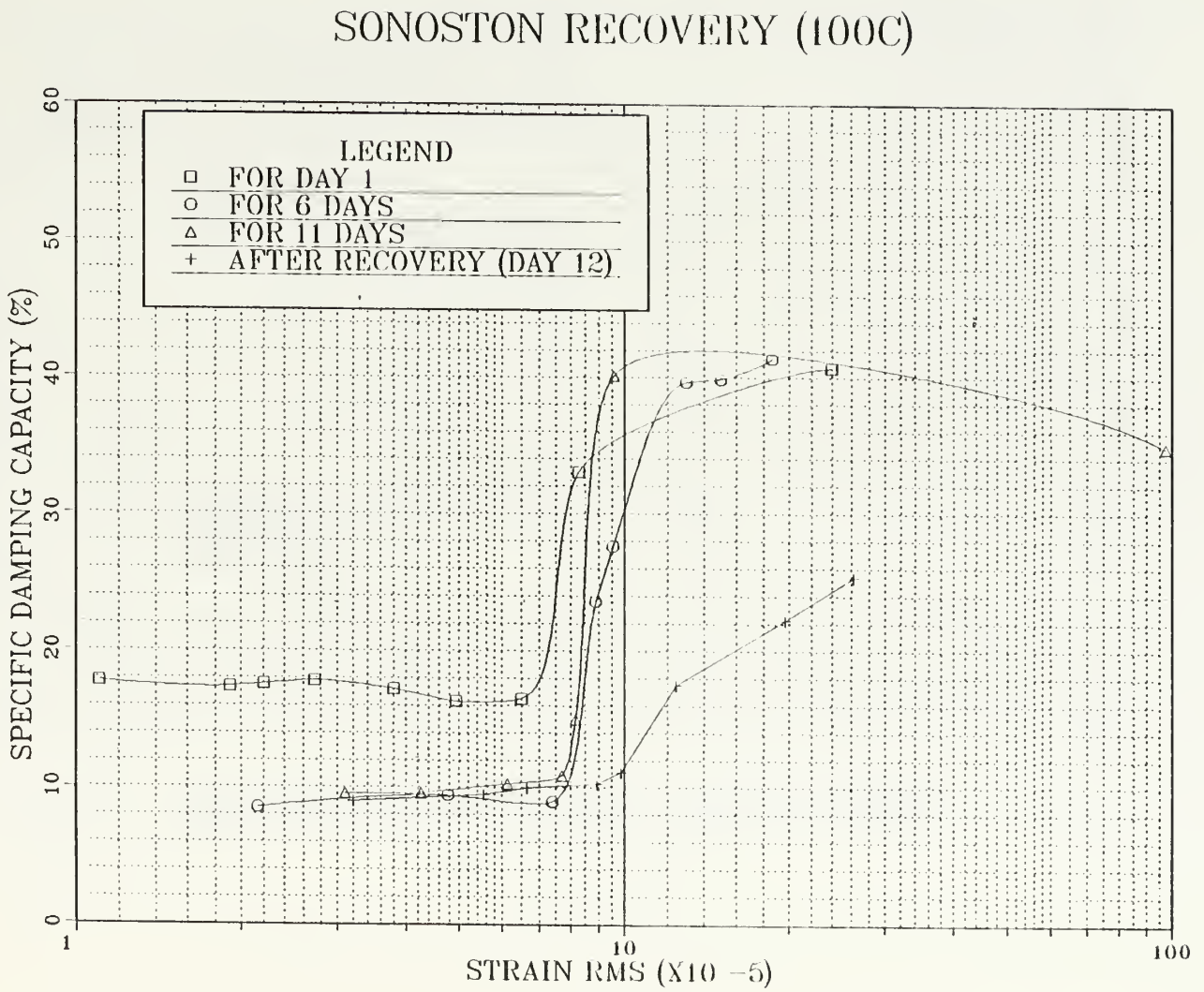
SONOSTON RECOVERY (100C)
LEGEND
FOR DAY 1
FOR 6 DAYS
FOR 11 DAYS
AFTER RECOVERY (DAY 12)
SPECIFIC DAMPING CAPACITY (%)
0
10
20
30
40
50
60
1
10
100
STRAIN RMS (X10 −5)

FIGURE 10.

INCRAMUTE RECOVERY (ROOM TEMP)

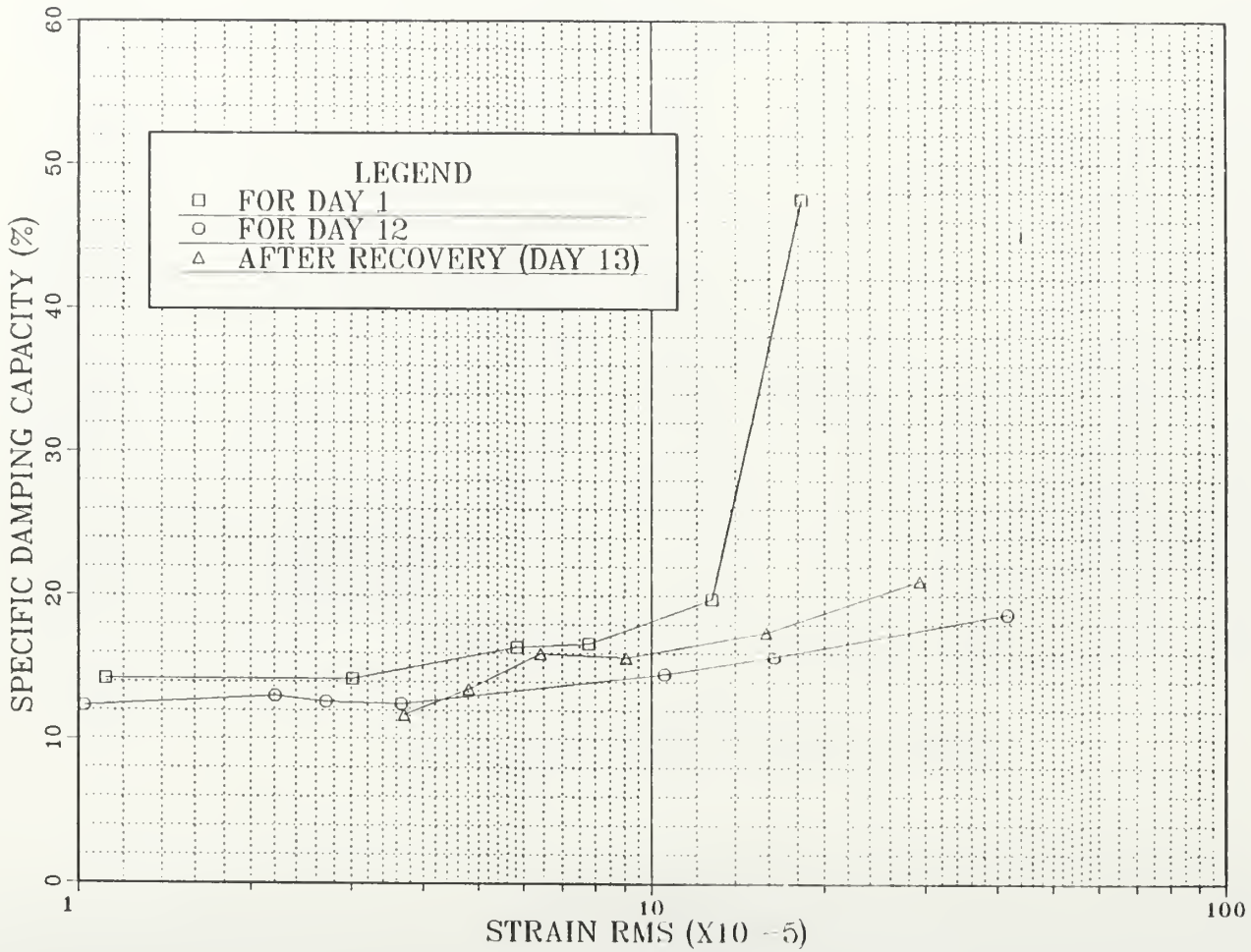

FIGURE 11.

INCRAMUTE RECOVERY (100C)

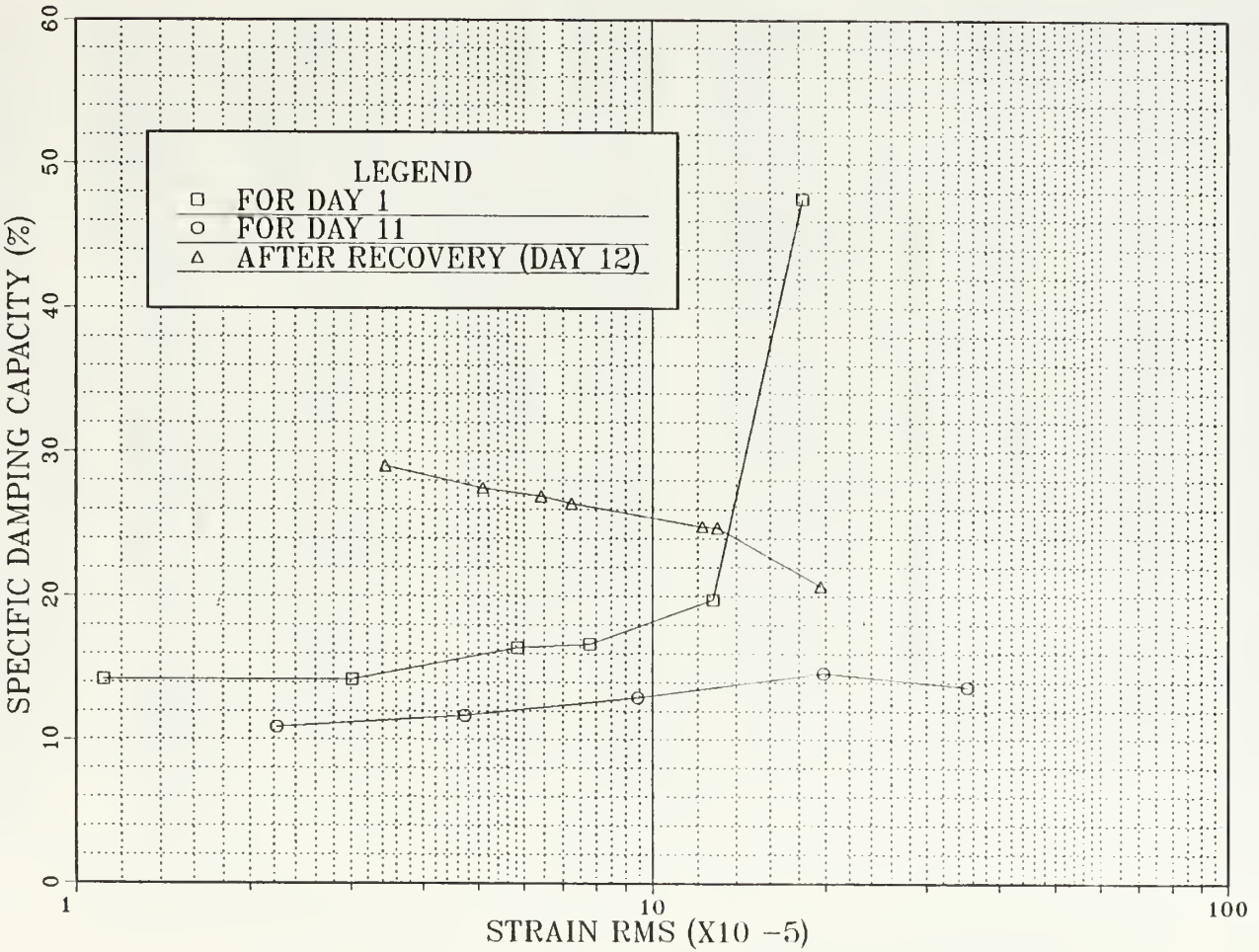

FIGURE 12.

INITIAL CYCLING STRAIN ANOMALY

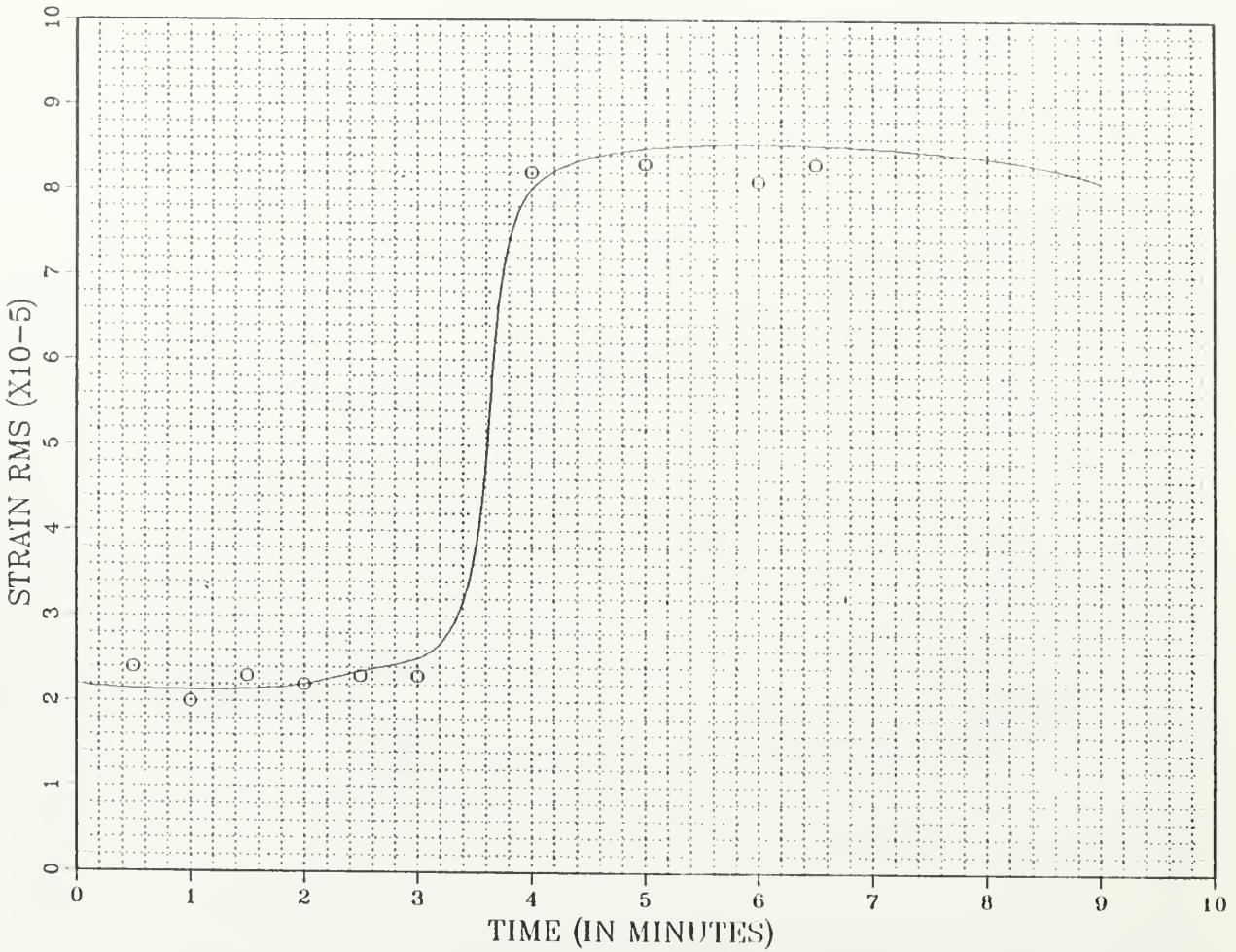

FIGURE 13.

LIST OF REFERENCES

1. Bert, C.W., "Material damping: An introductory review of Mathematical models,measures and experimental techniques," Journal of Sound and Vibration, Vol. 29, No. 2, pp. 129-153, 1973.

2. de Batist, R., Internal Friction of Structural Defects in Crystalline Solids, North-Holland Publishing Co., Amsterdam, 1972.

3. Reed-Hill, R.E., Physical Metallurgical Principles, Brooks/cole Engineering Div.,1973.

4. Thomson, W.T., Theory of Vibration with Applications, Prentice-Hall, Inc., 1981.

5. Ito, K. and Tsukishima, M., "Damping Capacity of $(Mn_{1-x}Co_x)_{0.95}Cu_{0.05}$ Metastable gamma Phase Alloys," Transactions of the Japan Institute of the Metals, Vol. 26, No. 3, pp. 319-324, 1985.

6. Birchon, D., Bromley, D.E., and Healey, D., "Mechanism of Energy Dissipation in high damping capacity Manganese-Copper alloys," Metal Science Journal, Vol. 2,pp. 41-46, 1968.

7. Sogabe, Y., Kishida, K., and Nakagawa, K., "Wave Propagation Analysis for Determining the Dynamic Properties of High Damping Alloys," Bulletin of the JSME, Vol. 25, No. 201, pp. 321-327, March 1982.

8. Dean, R.S., Long, J.R., Graham, T.R., Roberson, A.H., and Armantrout, C.E., "The Alpha Solid Solution of the Copper-Manganese-Aluminum System," Transactions of the AIME, Vol. 171, pp. 70-88, 1947.

9. Vintaykin, Y.Z., Litvin, D.F., and Udovenko, V.A., "Fine Crystalline Structure in Highly Shock-Absorbing Alloys of Manganese and Copper," Physics of Metals and Metallography, Vol. 37, No. 6, pp. 1228-1237, 1974.

10. Hedley, J.A., "The Mechanism of damping in Manganese Copper alloys," Metal Science Journal, Vol. 2, pp. 129-137, July 1968.

11. Vintaykin, Y.Z., Dmitriyev, V.B., and Udovenko, V.A., "Anti-ferromagnetism in Heterogeneous Manganese/Copper Alloys," Physics of Metals and Metallography, Vol. 44, No. 5, pp. 107-113, 1979.

12. Nittono, Satoh, and Koyama, "Cubic Tetragonal Transformation and Reversible Shape Memory Effect in Mn-Cu Alloys," Japan Institute Metals, Vol. 22, 1981.

13. Butler, E.P., and Kelly,P.M., "High Damping Capacity Copper alloys. Part I - Metallography," Transactions of the Metallurgical Society of AIME, Vol. 242, pp. 2099-2106, October 1968.

14. Vitek, J.M. and Warlimont, H., "On a Metastable Miscibility Gap in gamma Mn-Cu Alloys and the origin of their high damping capacity", Metal Science, Vol. 10. No. 1, pp. 7-13, January 1976.

15. Barsch, G.R. and Krumhansl, J.A.,"Twin boundaries in Ferroelastic Media Without Interface Dislocations," Physical Review Letters, Vol. 53, September 1984.

16. Wen, S.H., Khatchaturyan, A.G., and Morris Jr. J.W., "Computer Simulation of a 'Tweed Transformation" in an idealized plastic Crystal," Metallurgical Transactions A, Vol 12A, pp. 581-587, April 1981.

17. Onozuka, T., Ohnishi, N., and Hirabayashi, M., "Low Temperature Electron Microscopy on the cubic-tetragonal transformation of V_3Si,"(unpublished) presented at the 115th annual Meeting of The Metallurgical Society of the AIME at New Orleans, Louisiana, 2-6 March 1986.

18. Tanner, L.E., Pelton, A.R., and Gronsky, R., "The Characterization of Pretransformation Morphologies: Periodic Strain Modulations," Journal de Physique, Vol. 53, December 1982.

19. Yamada, Y. "Modulated Lattice Relaxation in Beta-based Pre-martensitic Phase," Unpublished paper. Undated.

20. Mukherjee, K., Chandrasekaran, M., and Milillo, F., "Pre-martensitic-martensite transitions related to shape memory effect," Polytechnic Institute of New York, date unknown.

21. Oshima, R., Sugiyama, M., and Fujita, F.E.,"Tweed Structure Associated with FCC-FCT Transformations in Fe-Pd Alloys," (unpublished) presented at the 115th annual Meeting of The Metallurgical Society of the AIME at New Orleans, Louisiana, 2-6 March 1986.

22. Fister,J.C. and Breedis,J.F., "Degradation and Recovery of Damping in Incramute," INCRA PROJECT No. 274, January 1978.

23. Butler, E.P. and Kelly,P.M., "High Damping Capacity Copper alloys. Part II - The effect of storage and Deformation on the damping capacity of 70/30 Mn-Cu alloy," Transactions of the Metallurgical Society of AIME, Vol. 242, pp. 2107-2109, October 1968.

24. Reskuvich, J., "Cyclic Strain Amplitude and Heat Treatment Effects on the High Damping Behavior of INCRAMUTE Alloy under Random Vibration Loading in the 50-1000 Hz Frequency Range," M.S. and M.E. Thesis, Naval Postgraduate School, Monterey, California, September 1986.

25. Bolt, Beranek and Newman, Inc., Cambridge, Massachusetts, "Operations Manual for the Bolt, Beranek, and Newman, Inc., Resonant Dwell Apparatus," January 1973.

INITIAL DISTRIBUTION LIST

		No. Copies
1.	Defense Technical Information Center Cameron Station Alexandria, Virginia 22304-6145	2
2.	Library, Code 0142 Naval Postgraduate School Monterey, California 93943-5002	2
3.	Department Chairman, Code 69Hy Department of Mechanical Engineering Naval Postgraduate School Monterey, California 93943-5002	1
4.	Professor A.J. Perkins, Code 69Ps Department of Mechanical Engineering Naval Postgraduate School Monterey, California 93943-5002	10
5.	Lt. Lewis W. Leary SWOSCOM, Bldg. 446, Class 97 Newport, R.I. 02841	1
6.	Mr. Robert Hardy, Code 2803 David W. Taylor Naval Ship Research Center Annapolis, Maryland 21402	5
7.	Ms. Cathy Wong, Code 2812 David W. Taylor Naval Ship Research Center Annapolis, Maryland 21402	5
8.	Mr. Dale T. Peters Technical Director, Metallurgy INCRA, 708 3rd Ave. New York, New York 10017	1

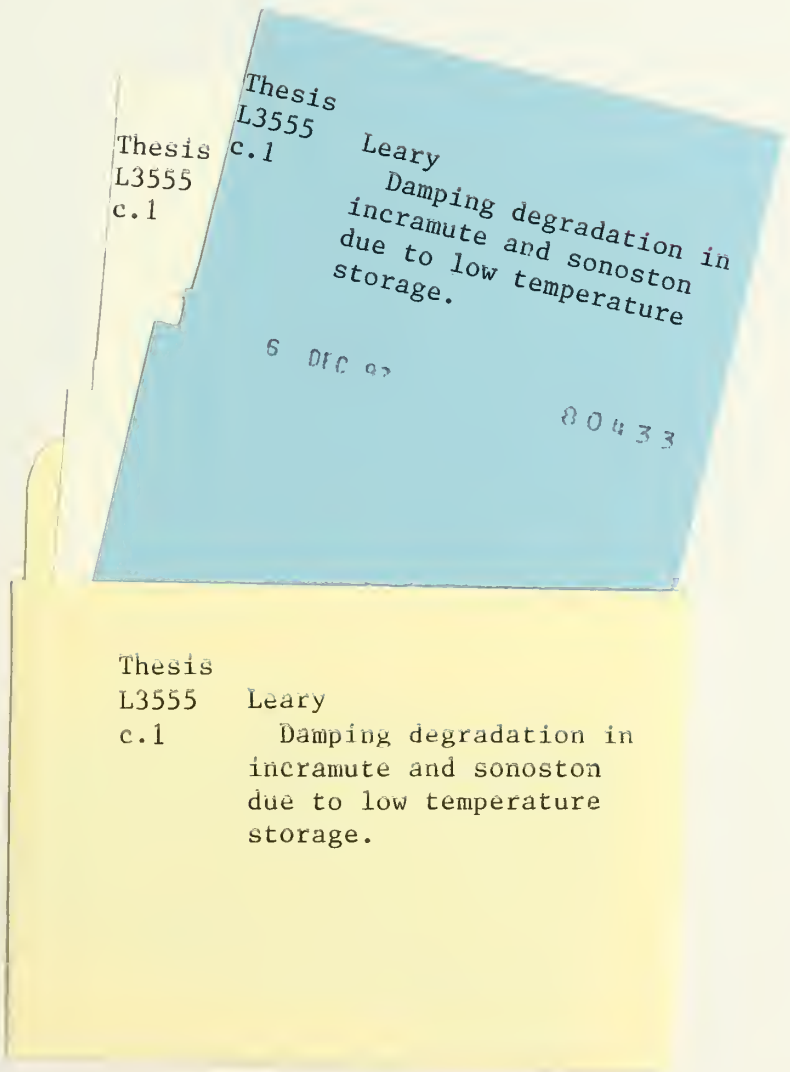

Thesis
L3555
c.1
Leary
Damping degradation in incramute and sonoston due to low temperature storage.